SOLVATED ELECTRON MODELS

BY

GEORGE HOWAT. B.Sc.

A thesis presented for the degree of
Doctor of Philosophy, at the
University of Glasgow.

Chemistry Department,
Glasgow University.

July 1972.

ProQuest LLC.
789 East Eisenhower Parkway
P.O. Box 1346
Ann Arbor, MI 48106 – 1346

ABSTRACT.

The theory of solvated electrons is traced from its early origins. The successes and limitations of these treatments are discussed. An alternative viewpoint, which considers the local interactions between the surplus electron and the molecules in its immediate environment, is developed. Dimeric and tetrameric models for the excess electron in water and ammonia are proposed and investigated by way of semi-empirical molecular orbital theory.

The peak positions calculated for the optical absorption spectrum of the electron in water, ammonia and ammonia-water mixtures are in fair agreement with experimental observations. Variations in peak position with pressure and temperature are in accord with experiment.

Dilation measurements are suggested to be better accomodated by a lattice expansion than by cavity formation.

Accounts of some of this work have been published in Ber. Bunsenges. phys. Chem., 75, 626 (1971), Radiation Reviews, (in press) and J. Phys. Chem., (in press).

ACKNOWLEDGEMENTS.

I should like to thank my supervisor, Dr.B.C. Webster for his help and enthusiasm, demonstrated throughout the course of this work.

I also thank my wife for her patience while preparing this manuscript.

Finally, I should like to thank the Carnegie Trust for my scholarship.

TABLE OF CONTENTS.

CHAPTER 1.

THE AIMS OF THE THEORY.

'... electrons are the atoms of the chemical element electricity...' This hypothesis was introduced by Sir William Ramsey in 1908 in order to represent some chemical phenomena. Since the previous year, when Kraus intimated that solutions of alkali metals in ammonia contain the solvated electron, the subsequent discoveries by research in this field can perhaps be considered to strengthem Ramsay's hypothesis.

Many of the phenomena exhibited by the surplus electron in a liquid are indeed analogous to those of an element, or at least, a unique chemical entity. For example the electron displays a typical optical absorption band shape and the properties of a well defined nucleophile.[1] Even more interesting are the observations that the volume associated with the electron and the absorption peak position vary considerably over a range of solvents.

The properties of solvated electrons have been the focus of concentrated investigation for some 70 years, leading to the detection of the hydrated electron in 1962.[2] That the electron is now known to exhibit many characteristic properties in liquids and solids is currently a matter of great theoretical and experimental interest.[3] In conjunction with the observation of new manifestations of the electron's prescence, the theoretical studies have advanced to a fairly sophisticated level, but many gaps in our understanding still exist.

It is unfortunate that the lack of information concerning the liquid state dictates that these theoretical treatments be based on model structures for the solvated electron. In this light, a comment made by Stoney may be considered to be apposite - ' A theory means a supposition which we hope to be true...'

Any attempt to account for all the properties of the surplus electron within one model appears to be a futile exercise. For example, metal-ammonia solutions exhibit cation-electron and electron-electron interactions and a transition to metallic behaviour as the alkali metal concentration is increased. By choice, we are concerned with the properties of low concentrations of trapped electrons in ammonia and water, where the interactions with other species present in the liquid may be ignored.

Within this concentration range, a selection from the manifold phenomena observed for excess electrons has recently been

advocated to be of prime importance.[4] A satisfactory theory should be capable of rationalising at least this limited choice of properties.

The five observations so chosen are concerned with the primary process, dilation phenomena, absorption spectra, induced electron migration and electron spin resonance spectra. These five areas provide a natural pathway for the development of the theory of solvated electrons. At one extreme the important processes occuring during stabilisation are sought, whilst at the other, the intimate interactions of the localised electrons with the surrounding medium nuclei require some consideration. This viewpoint leads the theory in a direction which emphasises the dynamic nature of the solvated electron.

The main features of these five observations are here introduced, and are discussed in greater detail where appropriate in Chapter 4.

Little is understood concerning the process occuring in the liquid prior to solvation of the electron. Sub-excitation electrons are considered to reach thermal energies in a time of the order of 10^{-13} sec.[5] Whether the electrons which escape geminate recombination then form their own trapping potential by polarisation or find some defect sites in the liquid and by molecular reorientation form a deeper well is still to be ascertained. Certainly, the measurements of the free-ion-pair yield by Freeman and Fadyah, which were shown to exhibit some correlation with the dielectric constant of the solvent,[6] suggest that solvation takes place at a time comparable with the dielectric relaxation time, τ.

The theory of Mozumder[7] holds that substantial neutralisation occurs in the time $0 - \tau$, if the distance of the electron from the parent ion is less than the distance achieved on thermalisation. To estimate this thermal length, the theoretical and the observed electron escape probabilities, assessed by the ratio of the free ion yield to the total ionisation yield, are equated. In water, where the escape probability is approximately 0.5, the thermal length increases from 27Å (296°K) to 35Å (273°K) as the relaxation time increases. In general, excepting ice, a smaller relaxation time decreases the thermal length. When multiple relaxation processes

can occur, for example in the alcohols, a variety of thermal lengths may be obtained, suggesting that the important mode of relaxation leading to stabilisation must be determined.[4] It is also to be recognised that microscopic relaxation times may be expected to differ from the macroscopic values, thereby limiting the utility of Mozumder's approach.

Once the trapped electron is established, other important properties are exhibited. From the effects of pressure on the equilibrium constant of the reaction,[8]

$$NH_2^- + \tfrac{1}{2}H_2 = NH_3 + e^-_{solv} ,$$

the volume increment associated with the ammoniated electron is assessed to be 84 ± 15 ml/mole at 240°K. Direct observation of this dilation on solution of alkali metals in ammonia lead to similar values of ~64 ml/mole,[9] 86.1 ml/mole [10] and 103.6 ml/mole.[11] These expansions correspond to the formation of a spherical void with a radius of the order of 3Å. That the volume requirements of the electron vary with solvent is demonstrated by measurements on the hydrated electron which place the volume increment at < 20 ml/mole[12] and more recently 1 - 6 ml/mole.[13]

Whether cavities are formed in the liquid or the density falls in the region of the localised electron, or both, is yet to be ascertained.

The optical absorption spectrum of the solvated electron in general consists of a broad featureless band with a high energy 'tail'. In only one instance, for trapped electrons in deuterated methyl cyanide crystals, has any vibrational coupling with the medium motion been detected in the band.[14] Pulse radiolysis of water shows that the optical absorption band of the hydrated electron is fully established in a time less than 10 picoseconds,[15] while in some alcohol glasses at 77°K the spectrum forms and moves to the blue on the micrsecond time scale.[16]

Increases in temperature and pressure shift the peak position to lower and higher energies respectively. The bandwidth is less susceptible to temperature variations.[17]

The excited state of the surplus electron in water appears to have a lifetime of less than 6 picoseconds and the view is expressed that the absorption band may be better interpreted as a photoionisation efficiency profile.[18]

While the excited state in ice has been demonstrated to be bound,[19] this does not appear to be the case in γ- irradiated alkaline glasses.

At 77°K the absorption maximum of the electron in alkaline glass lies at 590nm.[20] Photobleaching by light of shorter wavelengths than 590 nm moves the peak position to the red. With light of wavelength 700 nm, the spectrum moves to the blue. These observations may be interpreted if the view is taken that the electron resides in a variety of different traps and photo - excitation of the electron proceeds via an unbound or autoionising state so that electrons may be redistributed between different sites. In its essentials, this picture is corroborated by the recent observation of a photocurrent in γ-irradiated alkaline ice.[21]

Observations of hyperfine splittings in the ESR spectrum of the trapped electron in irradiated alkaline ices are few.[22] Hyperfine interactions with protons appear to be small, with a coupling constant of 4 - 5 gauss. For dilute metal solutions in amines and ammonia the interactions are modulated so quickly that the observed spectrum is usually comprised of a single narrow resonance.[23] The small and negative electron spin density at protons in ammonia and amines suggests that some spin polarisation mechanism is operative.

The importance of the molecular nature of the medium is evident in each of these five areas. In particular, the detection of spin densities at nuclei suggests that the molecular orbital technique may be useful to evaluate the importance of spin polarisation.

This thesis is concerned with the study of molecular models for the surplus electron in liquids and a fresh approach to the understanding of the properties outlined above is commenced. The current theories and their limitations are reviewed in Chapter 3.

The results of the molecular orbital calculations are discussed in Chapter 4. The molecular orbital methods and semi-empirical theories for open shell systems are reviewed in Chapter 2.

References to Chapter 1.

1. M. Anbar and E.J. Hart, J.Amer.Chem.Soc., 84, 4090 (1962).
2. E.J. Hart and J.W. Boag, J.Amer.Chem.Soc., 84, 4090 (1962).
3. T.P. Das, Adv.Chem.Phys., 4, 303 (1962);
Solutions Metal - Ammoniac, Ed. G. Lepoutre and M.J. Sienko, Benjamin, New York (1964);
F.S. Dainton, Endeavour, 26, 115 (1967);
D.C. Walker, Quart.Rev., 21, 79 (1967);
U. Schindewolf, Angew.Chem.Int.Ed.(English), 7, 190 (1968);
M.H. Cohen and J.C. Thompson, Adv.Phys., 17, 857 (1968);
E.J. Hart, Surv.Prog.Chem., 5 129 (1969);
R. Catterall and N.F. Mott, Adv.Phys., 18, 665 (1969);
J. Jortner, Actions Chimiques et Biologiques des Radiations, Ed. M. Haïssinsky, p7, Masson et Cie, Paris (1970);
K. Eiben, Angew.Chem.Int.Ed. (English), 9, 619 (1970);
E.J. Hart and M. Anbar, The Hydrated Electron, Wiley, New York, (1970);
G. Scholes, Ann.Rept.Chem.Soc., 67, 169 (1970);
J. Shankar, J.Indian Chem.Soc., 48, 97 (1971);
4. B.C. Webster and C. Howat, Rad.Rev. (in press)
5. M. Burton, K. Funibashi, R.R. Hentz, P.K. Ludwig, J.L. Magee, A. Mozumder, Transfer and Storage of Energy in Molecules Vol.1., Ed. G.M. Burnett and A.M. North, P.161 (1969).
6. G.R. Freeman and J.M. Fadyah, J.Chem.Phys., 43, 86 (1965).
7. A. Mozumder, J.Chem.Phys., 50, 3153,3162 (1969).
8. U. Schindewolf, R. Vogelsgesang and K.W. Boddekar, Angew.Chem.Int.Ed. (English), 8, 512 (1969).
9. W.L. Jolly, Prog. in Inorg.Chem., 1, 235 (1959).
10. W.N. Lipscomb, J.Chem.Phys., 21, 52 (1953).
11. J. Jortner, J.Chem.Phys., 30, 839 (1959).
12. U. Schindewolf, H. Kohrmann and G. Lang, Angew.Chem.Int.Ed. (English), 8 512 (1969).
13. R.R. Hentz and D.W. Brazier, J.Chem.Phys., 54, 2777 (1971).
14. L. Holloman, E.D. Sprague and F. Williams, J.Amer.Chem.Soc., 92 429 (1970).
15. M.J. Bronskill, R.K. Wolff and J.W. Hunt, J.Chem.Phys., 53, 4201 (1970).
16. J.T. Richards and J.K. Thomas, J.Chem.Phys., 53, 218 (1970); L. Kevan, J.Chem.Phys., 56, 838 (1972).

17. S. Arai and M.C. Sauer, J.Chem.Phys., 44, 2297 (1966);
R.K. Quinn and J.J. Lagowski, J.Phys.Chem., 73, 2326 (1969).
18. G. Kenney-Wallace and D.C. Walker, J.Chem.Phys.,
55, 447 (1971).
19. K. Kawabata, J.Chem.Phys., 55, 3672 (1971).
20. G.V. Buxton, F.S. Dainton, T.E. Lantz and F.P. Sargent,
Trans. Faraday Soc., 66, 2962 (1970).
21. I. Eisele, R. Lapple and L. Kevan, J.Amer.Chem.Soc.,
91, 6504 (1969);
I. Eisele and L. Kevan, J.Chem.Phys., 53, 1867 (1970).
22. J.E. Bennett, B. Miles and A. Thomas, Nature, 201, 919 (1964),
J.Chem.Soc., A 1393 (1967);
K. Ohno, I. Takemura and J. Sohma, J.Chem.Phys., 56, 1202 (1972).
23. R. Catterall, Metal-Ammonia Solutions, Ed. J.J. Lagowski and
M.J. Sienko, p. 105, Butterworths, London (1970).

CHAPTER 2.

THE SEMI-EMPIRICAL MOLECULAR ORBITAL METHOD.

A. Introduction.

As an alternative to the valence bond quantum mechanical approach to electronic structure calculations, Mulliken emphasised that the electrons in a molecule should be considered as belonging to the molecule as a whole.[1] This simple concept, coupled with the subsequent development of molecular orbital techniques, has laid the foundation upon which many chemical and physical properties of systems may be rationalised in terms of their electronic distributions. To draw on one example may suffice. The simple molecular orbital method developed by Hückel has provided a simple tool for the understanding of phenomena exhibited by planar conjugated hydrocarbons.[2] Such simple methods have been superceded but their contribution to chemical theory remains.

For many particle systems the Schroedinger equation cannot in general be solved. It is necessary to have recourse to approximations of which the most widely used is the self-consistent field (SCF) method developed by Hartree.[3] In an intuitive way, each electron is considered to move under the influence of an average field set up by the nuclei and other electrons. The Schroedinger equation for a closed shell system becomes of the form

$$H_{eff}(1)\,\phi_k(1) = e_k\,\phi_k(1) \qquad (1)$$

for each molecular orbital. H_{eff} is some effective Hamiltonian operator, ϕ_k is a one-electron wave function - an orbital and e_k the eigenvalue. The relationship between equation (1) and the Schroedinger equation can be demonstrated using the variation principle and an approximate total wave function written as an orbital product or determinant.[4] The determinant is a formal expression of the self consistent field model of electron distribution.

In general, the accurate wave function is a linear combination of determinants, the first and dominant terms being made use of in molecular orbital theory. Since the fields exerted by the electrons are averaged, a single wave function will always neglect the instantaneous interactions of the electrons. The subsequent error in the calculated energy over the energy of the true solution to the unrelativistic Schroedinge equation is called the correlation energy. The effective Hamiltonian operator appearing in equation (1) may be shown to take the form

$$H_{eff}(1) = -\tfrac{1}{2}\nabla_1^2 - \sum_i Z_i/r_{1i} + \int \sum_j r_{12}^{-1}(2\,\phi_j^*(2)\,\phi_j(2) - \phi_j^*(2)\,\phi_j(1)P_{12})dv_2$$

which illustrates the averaging procedure. P_{12} is a permutation operator which permutes electrons 1 and 2. The conventional coulomb and exchange operators are defined as

$$J_j = \int \phi_j^*(2)\ \phi_j(2)/r_{12}\ dv_2$$

$$K_j = \int \phi_j^*(2)\ \phi_j(1)P_{12}/r_{12}\ dv_2,$$

so that the effective Hamiltonian operator is

$$H_{eff}(1) = -\tfrac{1}{2}\nabla_1^2 - \sum_i Z_i/r_{1i} + \sum_j (2J_j - K_j).$$

Since the systems of interest, excess electron states, contain an odd number of electrons, modifications in the theory described are required.

B(i) Open-Shell Molecular Orbital Theory.

The SCF theory of open shell systems is beset with difficulties not found in closed shell theory especially when a degenerate configuration is investigated. In such cases the trial wave function cannot be identified with a single determinant. Even if a convenient energy expression may be written, the system may not be described by a set of single particle equations having the simplicity of relation (1).

Consider the general form of equation (1):

$$H_{eff}(1)\ \phi_k(1) = \sum_j \phi_j e_{jk}.$$

The off-diagonal multipliers e_{jk}, $j \neq k$, are introduced in the variation calculation to ensure the orthogonality of the orbitals ϕ_j and ϕ_k. By a unitary transformation of these molecular orbitals among themselves the e_{jk} can be eliminated in closed shell theory. In general the open shell theory is complicated by the fact that all these multipliers cannot be simultaneously destroyed; consequently the equations are not unique.[5]

Three main methods of handling these off-diagonal multipliers exist. The first, described by Roothaan is called the combined Hamiltonian method.[5]

Commencing from the energy expression for an open shell system, each orbital is subjected to the variation $\phi_i \rightarrow \phi_i + \delta\phi_i$. Minimisation of the energy, subject to the constraint that orbitals form an orthonormal set, leads to two coupled SCF equations

$$F^c \phi_k = \sum_l \phi_l e_{lk} + \sum_n \phi_n e_{nk}$$

$$fF^o \phi_m = \sum_l \phi_l e_{lm} + \sum_n \phi_n e_{nm}.$$

The subscripts k,l and the superscript c refer to the orbitals within the closed shell while l,m and o denote the open shell. F^c and F^o are some operators the form of which need not be reproduced; f is the fractional occupation of the open shell.

By unitary transformations of the orbitals, the off-diagonal multipliers within each shell may be annihilated, but not those coupling open and closed shell orbitals. Roothaan showed how the absorption of the off-diagonal multipliers into some single effective Hamiltonian leads to a single eigenvalue equation of the form (1). The subsequent interpretation of the eigenvalues is not easy. In general they cannot be equated with ionisation potentials for the removal of an electron from a molecular orbital.

Alternatively, the problems arising from the multipliers may be sidestepped completely. In Nesbet's method, it is proposed that the molecular orbitals be calculated via a suitably chosen effective Hamiltonian.[6]

Electrons are constrained to occupy an orbital set in such a way that the total wave function can satisfy spin and symmetry requirements. The molecular orbitals are obtained as solutions of an arbitary set of equations taking the form

$$(H + \sum_j J_j - \sum_j' K_j) \phi_i = e_i \phi_i.$$

The summation over K_j runs over those orbitals with alpha spin factor. Utilising the aufbau principle, electrons are paired in orbitals - a spin equivalence restriction.

Unfortunately, the effective Hamiltonian may not conform to the form of the assumed wave function. Consequently, the energy is not the Hartree - Fock energy and as such is not an absolute minimum. In addition, the best form for the SCF equations may not be obvious, the choice of equations necessarily entails some degree of arbitrariness. Further improvements can be made by the inclusion of configuration interaction effects. Such calculations may be lengthy since Brillouin's theorem concerning the matrix elements of the Hamiltonian operator between mono-excited states and the ground state does not hold.[7] Brillouin's theorum states that the matrix elements of the Hamiltonian between the

ground and excited configurations obtained by replacing one Hartree-Fock orbital in the ground state by one of the virtual orbitals is zero ie.

$$\langle \Phi' | H | \Phi \rangle = 0$$

For ease of interpretation and improvement of the wave function, the unrestricted Hartree-Fock method (UHF) for open shell systems might be the best to use. This technique is used in the calculations to be described in chapter 4 and is dealt with more fully.

(ii) The Unrestricted Hartree - Fock Method.

The electrons of alpha spin in a system of non-zero spin suffer a different exchange potential from that of the beta spin electrons.[8] As a result, the spatial orbitals occupied by electrons of opposite spin will differ. This effect is termed 'spin polarisation'. In addition, permitting distinct spatial factors in the orbitals of a closed shell system represents the tendency of electrons to avoid each other. In short, some correlation between the electronic motions is introduced. Constraining particular orbitals to be doubly occupied is not a priori justified. It is often convenient.

For an N electron system, the electrons may be assigned to a set of orthonormal spin orbitals, p of the form $\phi\alpha$ and q of the form $\phi\beta$. The trial wave function for a variational calculation of the energy may be constructed as the single determinant

$$\Phi = (N!)^{-\frac{1}{2}} \det(\phi_1(1)\,\alpha(1) \ldots \phi_p(p)\,\alpha(p)\,\phi_{p+1}(p+1)\,\beta(p+1) \ldots), \qquad (2)$$

in which no restrictions are imposed on the form of the spatial parts of the one-electron functions. This determinantal wave function is not an eigenfunction of the total spin operator S^2 (ref.9) ie.

$$\langle S^2 \rangle_{av} = \tfrac{1}{4}(p-q) + \tfrac{1}{2}(p+q) - \sum_{i}^{p} \sum_{j}^{q} \int \phi_i(1)\, \phi_i^*(2)\, \phi_j^*(1)\, \phi_j(2) dv_1 dv_2$$

Only in the special case when q orbitals are doubly occupied ($p \geq q$) is this Φ an eigenfunction of S^2.

The expectation value of the energy is given by the expression

$$E = \frac{\langle \Phi | H | \Phi \rangle}{\langle \Phi | \Phi \rangle}$$

$$= \sum_i H_{ii} + \tfrac{1}{2}\Big(\sum_{ij} J_{ij} - \sum_{ij}{}' K_{ij} \Big). \qquad (3)$$

The summation over K_{ij} is limited to between orbitals of the same spin factor. The one electron integral H_{ii}, the coulomb integral J_{ij}, and the exchange integral K_{ij} are given by

$$H_{ii} = \int \phi_i^*(1) \left\{ -\tfrac{1}{2} \nabla_1^2 - \sum_k Z_k / r_{1k} \right\} \phi_i(1)\, dv_1 = \int \phi_i^*(1)\, H\, \phi_i(1)\, dv_1$$

$$J_{ij} = \int \phi_i^*(1)\, J_j\, \phi_i(1)\, dv_1$$

$$K_{ij} = \int \phi_i^*(1)\, K_j\, \phi_i(1)\, dv_1 .$$

When the energy is minimised, the orbitals in each set must satisfy the SCF equations

$$(H + \sum_j^N J_j - \sum_l^p K_l)\, \phi_i = \sum_l^p \phi_l e_{li} \qquad i=1,2....p$$

$$(H + \sum_j^N J_j - \sum_l^q K_l)\, \phi_i = \sum_l^q \phi_l e_{li} \qquad i=p+1,...N.$$

No Lagrangian multipliers e_{li} coupling the two sets of orbitals are introduced since the solutions of the two equations are automatically orthogonal by virtue of the spin factors. Eliminating the off-diagonal multipliers by transforming the orbital sets reveals two sets of equations of the form (1),

$$(H + \sum_j^N J_j - \sum_l^p K_l)\, \phi_i^\alpha = e_i^\alpha \phi_i^\alpha$$

$$(H + \sum_j^N J_j - \sum_l^q K_l)\, \phi_i^\beta = e_i^\beta \phi_i^\beta ,$$

which are linked by a common coulomb potential.

It may be shown that the solutions of this set of equations do satisfy Koopmans[10] and Brillouins theorems.

The advantage of the UHF method lies in the simplicity of calculation for open shell systems, but Löwdin focuses attention on several objections to the method.[9]

Albeit that the magnitude of the orbital splitting is dependent on the correlation between electron motions, systems with unbalanced spin exhibit the exchange or spin polarisation effect. Doubts may be cast questioning the accuracy of the UHF method for the evaluation of such effects. Can a wave function which is not an eigenvalue of S^2 adequately describe properties arising from electron spin?

Theoretically, the energy calculated with an unrestricted wave function will be lower than that calculated by the Roothaan method. As the orbital splitting increases, the single determinantal function approximates less to that for a pure spin state.

Eventually the contribution from higher multiplicities may balance any lowering in energy by further orbital splitting. No improvement will be observed.

If the desired multiplicity is 2s+1, the unwanted contaminants may be removed from Φ by application of the projection operator[11]

$$\Lambda = \prod_{k \neq s} \frac{S^2 - k(k+1)}{s(s+1) - k(k+1)}.$$

Löwdin recommends that a trial function $\Lambda\Phi$ be utilised to calculate the energy. The computations become formidable. For approximate calculations it may be sufficient to apply the projection operator after the calculation of the best single determinantal wave function. Amos and Hall derived the formula for the energy after destruction of the principal contaminant, the lowest unwanted multiplicity.[12] The underlying conditions upon which some benefit is obtained by projection are not clear.[13]

Of the three techniques described, the UHF scheme supplies the least complicated avenue to an approximate open shell wave function. In the study of hyperfine interactions the method is invaluable.[14]

C. The Matrix Formulation of the UHF Method.

The spherical symmetry of atoms lends simplicity to the solution of the Hartree-Fock equations. No analytic form need be imposed on the one-electron orbitals. For molecular problems, it is more convenient to express each orbital ϕ_i as a linear combination of some set of basis functions X,

$$\phi_i = \sum_j X_j C_{ji}. \qquad (4)$$

Collecting the coefficients into a column vector $\underline{C}_i$, this equation may be written $\phi_i = \underline{X}\,\underline{C}_i$. If $\underline{C}$ is the array whose i'th column is $\underline{C}_i$, the molecular orbitals may be collected in the form

$$\underline{\phi} = \underline{X}\,\underline{C}.$$

If the expansion (4) is to be exact, the basis set must be complete. For practical reasons, a truncated basis set must be used, the size being dictated by the accuracy in the energy required and the

computer to be used. Appropriate atomic orbitals centred on each atom in the molecule are chosen to synthesise the molecular orbitals, although the work of Whitten emphasises that this need not be the case.[15] The orbital centres may also be allowed to 'float' over the molecular framework to positions for which the energy is lowest.[16]

When the expansion technique is used, the search for the best molecular orbitals involves the manipulation of matrices. To each one-electron operator A is assigned the matrix $\underline{A}$ with elements A_{ij} calculated as

$$A_{ij} = \int \chi_i^* \, A \, \chi_j \, dv.$$

In particular, the overlap matrix elements are

$$S_{ij} = \int \chi_i^* \, \chi_j \, dv.$$

In matrix notation, the orthonormality condition for the molecular orbitals is

$$\underline{C}_i \, \underline{S} \, \underline{C}_j = \delta_{ij},$$

assuming that the molecular orbital coefficients are real.

For the unrestricted single determinantal wave function (2), the expectation value of the energy (3) is

$$E = \sum_i \underline{C}_i \, \underline{H} \, \underline{C}_i + \sum_{i<j} \underline{C}_i \, \underline{J}_j \, \underline{C}_i - \sum_{i<j} \underline{C}_i^{\alpha} \, \underline{K}_j^{\alpha} \, \underline{C}_i^{\alpha} - \sum_{i<j} \underline{C}_i^{\beta} \, \underline{K}_j^{\beta} \, \underline{C}_i^{\beta}$$

where $\underline{C}_i^{\alpha}$ and $\underline{K}_j^{\alpha}$ are the molecular orbital coefficient vectors and the exchange operator matrices for alpha spin respectively.

When this energy is a minimum, any infinitesemal change in the molecular orbitals, tantamount to altering the vectors $\underline{C}_i$ by an increment $\delta\underline{C}_i$, the energy is raised. Constraining any such variations to preserve the orthonormality of the orbitals implies that

$$\delta\underline{C}_i \, \underline{S} \, \underline{C}_j + \underline{C}_j \, \underline{S} \, \delta\underline{C}_i = 0$$

for each pair of orbitals i and j. Recognising that each of the alpha spin orbitals is automatically orthogonal to all the beta spin orbitals, the variation in energy on altering one of the alpha spin orbitals is

$$\delta E = \delta\underline{C}_i^{\alpha} \left\{ \left[H + \sum_j J_j - \sum_j K_j^{\alpha} \right] \underline{C}_i^{\alpha} - \sum_j \underline{S} \, \underline{C}_j^{\alpha} \, e_{ji}^{\alpha} \right\} + \text{c.c.}$$

Lagrangian multipliers e_{ji}^{α} are introduced as described in the previous section. The symbol c.c. stands for the complex conjugate expression.

If the Hartree-Fock operator for alpha electrons is defined by

$$F^{\alpha} = H + \sum_{j}^{N} J_j - \sum_{j}^{P} K_j^{\alpha},$$

the 'best' alpha spin molecular orbital coefficients satisfy the equation, for $\delta E = 0$,

$$\underline{F}^{\alpha}\underline{C}_i^{\alpha} = \Sigma\, \underline{S}\, \underline{C}_j^{\alpha} e_{ji}^{\alpha}.$$

The equation for the beta spin orbital coefficients is of the same form with the alpha superscript changed to beta. Annihilating the off-diagonal multipliers displays the familiar secular equation form

$$(\underline{F}^{\alpha} - e_i^{\alpha}\, \underline{S})\underline{C}_i^{\alpha} = 0$$
$$(\underline{F}^{\beta} - e_i^{\beta}\, \underline{S})\underline{C}_i^{\beta} = 0.$$

These equations become identical when the wave function (2) represents a pure singlet state.

The secular equations (5) show that one has to deal with two sets of simultaneous equations which are coupled.

The difficulties which have plagued the investigator of electronic structures lie in the construction of the F matrices. Every element of the Hartree-Fock matrix involves the computation of two electron integrals, viz.

$$(pq/rs) = \int \chi_p(1)\, \chi_q(1) r_{12}^{-1}\, \chi_r(2)\, \chi_s(2)\, dv_1 dv_2,$$

$$F_{pq} = H_{pq} + \sum_{r,s} P_{rs}\, (pq/rs) - P_{rs}^{\alpha}\, (ps/rq), \qquad (6)$$

where the one electron density matrices P^{α}, P are obtained from the molecular orbital coefficients.

$$P_{rs}^{\alpha} = \sum_{i}^{P} C_{ri}^{\alpha}\, C_{si}^{\alpha} \qquad P_{rs}^{\beta} = \sum_{i}^{Q} C_{ri}^{\beta} C_{si}^{\beta} \qquad P_{rs} = P_{rs}^{\alpha} + P_{rs}^{\beta}.$$

Each of the basis functions may be centred on different nuclei present in the system, and the integral (pq/rs) becomes extremely difficult and tedious to calculate. When the basis set is large, more time may be spent in calculating these integrals than in the steps towards obtaining the molecular orbital coefficients.

Constructing a basis set from Gaussian orbitals facilitates this calculation,[17] but large numbers of basis orbitals must be utilised. The ease of computation is offset by the problem presented by efficient

storage of these integrals.

With the advent of larger and faster computers, it should soon be a routine matter to perform ab initio calculations on fairly large molecules. However, this was not always the case, and a large body of simplified methods based on the secular equations (5) has grown up. Approximate calculations were viewed to be better than none at all.

D. The Semi-Empirical Techniques and the INDO Method.

The impetus to investigate chemical phenomena by way of quantum mechanical calculations is great. Yet this should only be performed with an economy of effort, enough to reveal the salient features where accurate evaluation of a property is precluded. Semi-empirical molecular orbital techniques provide such a ready tool. These schemes, based on the equations (5), lie within a spectrum of complexity rangeing from ab initio through to the simple Hückel treatment for planar hydrocarbons, the particular technique for use being suggested by the problem. The success of naive schemes and the recognition that refinements usually lead to poorer agreement between theory and experiment has led to speculation as to whether the Hartree-Fock scheme really represents the fundamental basis for these semi-empirical theories.[18]

In essence, semi-empirical schemes rely on the plausability of constructing a theory to simulate the accurate calculation by sole consideration of the quantities likely to be important in a full treatment. It follows that any satisfactory theory should exhibit the properties of the Hartree-Fock solutions, particularly the invariancy properties. That is, the total wave function and energy must be invariant to unitary or orthogonal transformations of the molecular orbitals among themselves,[4] or to any such transformation of the basis set orbitals. Preservation of this property enforces other approximations.[19] For example, in the neglect of all two-electron integrals involving overlap charge densities, $\chi_p(1)\,\chi_q(1)$, it is imperative that the remaining integrals are independent of orbital type. This is the criterion used to construct the Complete Neglect of Differential Overlap method, (CNDO).[20] Approximate methods invariably neglect, estimate or do not consider at all, some two-electron integrals,

arguing that their effects are only marginal.

The approximations invoked should not be so severe that the predictions made by the method are at variance with experience. The CNDO method predicts that the singlet and triplet states of the linear CH_2 radical are degenerate, the triplet should be more stable. The inclusion of single centre exchange integrals rectifies this fault, giving rise to the Intermediate Neglect of Differential Overlap method (INDO).[21] Retention of these exchange integrals is important for calculations on systems with non-zero spin.

Many semi-empirical methods are available,[22] but the success achieved by the INDO method for open shell systems recommends its use for the study of solvated electron models, and the approximations are here laid out in detail.

(ii) The INDO Approximations.

(a) By virtue of their relatively small spatial extension and low energy, it is reasonable to assume that the inner shell electrons form part of an unpolariseable core of charge $Z_A = Z'_A - n$, where Z'_A is the nuclear charge and n is the number of non-valence electrons. The one-electron operator matrix elements become

$$H_{pq} = \int \chi_p(1) \left\{ -\tfrac{1}{2}\nabla_1^2 - \Sigma V_A(r) \right\} \chi_q(1)\, dv_1 \qquad (7)$$

where $V_A(r)$ is the electrostatic field of the core of atom A. The core-core interaction energy is approximately $\sum_{A<B} Z_A Z_B / R_{AB}$.

(b) Multicentre integrals (pq/rs) are in general small when overlap charge distributions are involved. The INDO method retains only the integrals involving differential overlap of basis orbitals on the same centre, all others are neglected. Choosing a basis set of the s,p,d... type ie. not hybrid orbitals, the remaining integrals are of the sorts (pp/pp), (pq/pq), $p \neq q$ on the same centre, and (pp/qq). Two-centre integrals of the latter form must be assumed independent of orbital type in order to preserve the invariancy conditions described in the previous section. In such cases, $G_{AB} = (pp/qq)$, is therefore dependent only on the nature of atoms A and B. This integral is estimated to have a magnitude given by the coulomb repulsion integral between the valence s orbitals on atoms A and B.

(c) To be consistent with the approximations set out in (b), the basis set is assumed to be orthonormal.

(d) The diagonal elements of the H matrix from equation (7) may be written

$$H_{pp} = \int \chi_p(1) \left[-\tfrac{1}{2}\nabla_1^2 - V_A(r)\right] \chi_p(1) dv_1 - \sum_{B \neq A} \int \chi_p(1) V_B(r) \chi_p(1) dv$$

$$= U_{pp} - \sum_{B \neq A} (p\ V_B\ p)$$

where p is centred on A. The quantity U_{pp} is an atomic parameter and is estimated from experimental data. The term $(p\ V_B\ p)$ represents the attraction of an electron in the orbital p for the core of B, and is approximated by

$$(p\ V_B\ p) = Z_B\ G_{AB}.$$

The off-diagonal matrix elements between orbitals on the same centre,

$$H_{pq} = U_{pq} - \sum_{B \neq A} (p\ V_B\ q)$$

are zero; U_{pq} by symmetry (s,p,d... basis set) while $(p\ V_B\ q)$ involves the core interaction with a differential overlap density on another centre and are neglected.

When orbitals χ_p and χ_q lie on different centres, A and B, the sole remaining term is

$$H_{pq} = \int \chi_p(1) \left[-\tfrac{1}{2}\nabla_1^2 - V_A - V_B\right] \chi_q(1) dv_1.$$

This "resonance integral" is a measure of the lowering of energy levels by the introduction of an electron into the attractive field between two cores. To satisfy invariancy conditions, it must be assumed that this element is independent of the orbital types on atoms A and B. The magnitude of H_{pq} is taken to be proportional to the overlap integral S_{pq} with a proportionality constant assumed to be the mean of two atomic quantities B_A and B_B. The overlap integrals are computed using Slater orbitals centred on each atom.

$$H_{pq} = \tfrac{1}{2}(B_A + B_B) S_{pq} = B_{AB}\ S_{pq}$$

(e) Utilising these approximations the Hartree-Fock matrix elements (6) are reduced to the relations

$$F^a_{pp} = U_{pp} + \sum_r^A P_{rr}(pp/rr) - P^a_{rr}(pr/pr) + \sum_{B \neq A} (P_{BB} - Z_B) G_{AB}$$

$$F^{a}_{pq} = (2P_{pq} - P^{a}_{pq})\,(pq/pq) - P^{a}_{pq}\,(pp/qq) \qquad p \neq q \text{ both on A}$$

$$F^{a}_{pq} = B_{AB}\,S_{pq} - P^{a}_{pq}\,G_{AB} \qquad p \neq q,\ p \text{ on A},\ q \text{ on B}.$$

where P_{BB} is the electronic charge on atom B given by

$$P_{BB} = \sum_{r}^{B} P_{rr}.$$

Comparison of these equations with the ab initio matrix elements (6) demonstrates the considerable simplification achieved by adopting the INDO approximations. The remaining problem lies in the appropriate choice of the parameters.

(iii) The Parametrisation of the INDO Method.[21]

The core integrals U_{pp} may be related to the ionisation potential and the electron affinity of the average atomic states of the isolated atom. Single centre repulsion integrals may be estimated from experimental spectral data. In this work, these integrals have been computed exactly.[23] The B_A parameters have been selected by Pople et al[21] to give the best overall fit with accurate limited basis set molecular orbital calculations on diatomic molecules. The parameters used in the calculations are collected in Table 1.

Table 1. The parameters used in the INDO calculations.

Atom	H	O	N
Orbital Exponent	1.2	2.275	1.95
$-B_A$(a.u.)	0.3307635	1.1392965	0.9187875
U_{ss}(a.u.)	-0.638729	-5.153006	-3.695835
U_{2p2p}(a.u.)		-4.661061	-3.296007
Z_A	1.0	6.0	5.0

An ALGOL computer program to perform these INDO calculations was written for the KDF9 computer at Glasgow.

As a comparison between the INDO calculation and a full limited basis set ab initio calculation, the charge density-bond order matrices computed for the water molecule are shown in Table 2. The matrix from the ab initio calculation has been transformed using

TABLE 2

The charge density-bond order matrices computed for the water molecule by the INDO method and an ab initio SCF method. The y-axis is perpendicular to the plane of the molecule, the z-axis is directed between the two protons. R(O-H) = 0.958A, HOH = 104.45°.

Ab initio

	O_{1s}	O_{2s}	O_{2px}	O_{2py}	O_{2pz}	H_{1s}	H_{1s}
O_{2s}	0.065	1.607	0.000	0.000	-0.372	0.495	0.495
O_{2px}	0.000		1.217	0.000	0.000	-0.690	0.690
O_{2py}	0.000			2.000	0.000	0.000	0.000
O_{2pz}	0.061				1.648	0.468	0.468
H_{1s}	-0.081					0.769	-0.014
H_{1s}	-0.081						0.769
O_{1s}	1.989						

INDO

	O_{2s}	O_{2px}	O_{2py}	O_{2pz}	H_{1s}	H_{1s}
O_{2s}	1.736	0.000	0.000	-0.355	0.407	0.407
O_{2px}		1.226	0.000	0.000	-0.689	0.689
O_{2py}			2.000	0.000	0.000	0.000
O_{2pz}				1.522	0.549	0.549
H_{1s}					0.758	-0.016
H_{1s}						0.758

Löwdin's orthoganalisation procedure[24] to that appropriate to an orthonormal basis set for the comparison between the two calculations. The basis set is that devised by Palmer and Gaskell.[25]

Although the INDO calculation does not include the core orbitals, the fit is seen to be quite good.

E. The Calculation of the Excitation Energies.

A facility for the calculation of excitation energies was included in the computer program.

Making the assumption that little orbital reorganisation takes place on excitation, this is a relatively simple computation. The highest occupied molecular orbital is vacated and the electron is promoted to the lowest unoccupied virtual orbital. The excited state energy is then calculated in the usual manner.

The restriction that little orbital reorganisation takes place on excitation is important. When the electron shifts are extensive, the ground state orbitals and the virtual orbitals are no longer good approximations to the excited state orbitals. More involved procedures are required. Extensive configuration interaction or a full SCF calculation on the excited state may be necessary.[26]

References to Chapter 2.

1. W. Heitler and F. London, Z.Physik, 44, 455 (1927);
   R.S. Mulliken, Phys.Rev., 82, 186,388,761 (1928).
2. E. Hückel, Z.Physik, 70, 204 (1931).
3. D.R. Hartree, The Calculation of Atomic Structures, Wiley,
   New York (1957).
4. V. Fock, Z.Physik, 61, 126 (1930),
   J.C. Slater, Phys.Rev., 35, 210 (1930).
5. C.C.J. Roothaan, Rev.Mod.Phys., 32, 179 (1960).
6. R.K.Nesbet, Proc.Roy.Soc. (London) A230, 312 (1955).
7. L. Brillouin, Actualites sci. et ind. No. 71 (1933).
8. D.R. Hartree, Proc.Roy.Soc. (London) A154, 588 (1936).
   J.C. Slater, Phys.Rev. 82, 538 (1951).
9. P-O. Löwdin, Adv.Chem.Phys., 2, 207 (1959).
10. T. Koopmans, Physica, 's Grav., 1, 104 (1933).
11. P-O. Löwdin, Phys.Rev., 97, 1509 (1955).
12. A.T. Amos and G.G. Hall, Proc.Roy.Soc. (London), A263
    483 (1961), A.T. Amos, Mol.Phys., 5, 91 (1962).
13. G. Berthier, in P-O. Löwdin and B. Pullman (Eds),
    Molecular Orbitals in Chemistry, Physics and Biology,
    p. 57, Academic Press, New York, 1964.
14. H.M. McConnell and D.B. Chesnut, J.Chem.Phys., 28, 107 (1958).
15. J.L. Whitten, J.Chem.Phys., 39, 349 (1963).
16. A.A. Frost, B.H. Prentice and R.A. Rouse, J.Amer.Chem.Soc.,
    89, 3064 (1967).
17. S.F. Boys, Proc.Roy.Soc. (London), A200, 542 (1950).
18. P-O. Löwdin, Ref. 13, p.37.
19. J.A.Pople, D.P. Santry, G.E. Segal, J.Chem.Phys., 43, S129 (1965).
20. J.A. Pople, G.A. Segal, J.Chem.Phys., 44, 3289 (1966).
21. J.A. Pople, D.L. Beveridge and P.A. Dobosh, J.Chem.Phys., 47,
    2026 (1967)
    J.A. Pople and D.L. Beveridge, Approximate Molecular Orbital
    Theory, McGraw-Hill, New York (1970).
22. O. Sinanoglu and K.B. Wiberg, Sigma Molecular Orbital Theory,
    Yale Univ. Press, New Haven and London, (1970)
    B.J. Nicholson, Adv.Chem.Phys., 18, 249 (1970)
    W.G. Richards and J.A. Horsley, Ab Initio Molecular Orbital
    Calculations for Chemists, Oxford Univ.Press, London (1970).

23. M. Kotani, A. Amemiya, E. Ishiguro and T. Kimura, Tables of Molecular Integrals, Maruzen, Tokyo (1955).
24. P-O. Löwdin, J.Chem.Phys., 18, 365 (1950).
25. M.H. Palmer and A.J. Gaskell, Theor.Chim.Acta., 23, 52 (1971).
26. L.C. Cusachs and J.H. Corrington, ref. 22, p.256.

CHAPTER 3.

SOLVATED ELECTRON THEORY.

Introduction

Two basic conceptions dominate the theory of dilute solutions of surplus electrons in polar liquids. The first stresses the contribution of polarisation effects towards electron stabilisation while the second lays importance upon formation of void volumes at the localisation centre. Both facets are now incorporated into solvated electron theory. The development of the current models for electron stabilisation in polar media is traced.

A(i) The Importance of Polarisation.

Landau intimated that electrons in an ideal crystal may be stabilised at some locally deformed site if the total energy of the deformed crystal and electron is lower than that of a 'free' electron and the undeformed crystal.[1] The deformation is here associated with the prescence of the electron. Coulombic interactions between the lattice and the electron set up a polarisation field which Pekar identified with the trapping potential.[2]

Two distinct cases can be discerned. This polarisation either can or cannot follow the moving electron. In ionic crystals, where the displacement of ions creates a polarisation field, the latter case is important. Massive ions are unable to adjust their position fast enough to follow the electron motion. Consequently, this 'inertial polarisation' causes a force to act back upon the electron.

The potential well so formed localises the electron and is held by Pekar to be responsible fo both the deformation of the crystal as well as the electron stabilisation. Electrons in such states are termed 'polarons'.

(ii) The Theoretical Description of the Polaron.

When the localised electron in a crystal is distributed over a large region in the medium, the discrete lattice may be approximately replaced by a continuous dielectric medium. The polarisation at any point in the dielectric will be determined by the field

$$\underline{D}(r) = \int |\psi(r')|^2 \, (\underline{r} - \underline{r}')/|\underline{r} - \underline{r}'|^3 \, dv' \qquad (1)$$

where $\psi(r')$ is the wave function of the electron.

For a medium characterised by high and low frequency dielectric constants D_{op} and D_{st} respectively, the total polarisation created by the displacement $\underline{D}$ is

$$\underline{P}_t = (1 - 1/D_{st})\ \underline{D}/4\pi .$$

Since the electronic polarisation is described by

$$\underline{P}_e = (1 - 1/D_{op})\ \underline{D}/4\pi ,$$

the inertial polarisation which cannot follow the electron's motion is

$$\underline{P}_i = (\underline{P}_t - \underline{P}_e) = C\ \underline{D}/4\pi \qquad (2)$$

where $C = (1/D_{op} - 1/D_{st})$.

The energy of the electron in this polarisation field is given by the relation

$$E = 1/2m^* \int (\nabla \psi)^2\ dv + \int V\psi^2\ dv \qquad (3a)$$

$$= 1/2m^* \int (\nabla \psi)^2\ dv - \int \underline{P}_i \cdot \underline{D}\ dv \qquad (3b)$$

where m^* is the effective mass of the electron in atomic units and V is the potential energy acquired by the electron in a system of polarisation dipoles located at the lattice sites. Equation (3b) follows from equation (3a) when the lattice is replaced by a dielectric continuum, in which case,

$$V(r) = -C \int |\psi(r')|^2 / |\underline{r} - \underline{r}'|\ dv' \qquad (4)$$

Since the potential energy involves the wave function of the electron we have necessarily a self-consistent field problem.

To obtain the total energy of the crystal and electron, the energy E must be supplemented by the energy expended in inertially polarising the medium, $\frac{1}{2}\int \underline{P}_i \cdot \underline{D}\ dv$, and the energy of the electron in the conduction band of the unpolarised crystal.

Equations (3) may be solved by utilising the variation principle and some suitable approximate wave function. The lowest energy state has a wave function given by minimising the functional

$$J = 1/2m^* \int (\nabla \psi)^2\ dv - C/8\pi \int \underline{D}^2\ dv.$$

Employing a two-parameter variational function of the form

$$\psi = A(1 + ar + br^2)\exp(-ar), \tag{5}$$

Pekar showed that an upper bound to the energy, by minimising J is

$$E = -0.164m^*C^2 \tag{6}$$

associated with the optimised wave function

$$\psi = 0.1229a^{3/2} (1 + ar + 0.4516a^2 r^2) \exp (-ar)$$

$$a = 0.658m^*C$$

Photo-ejection of the electron from the localisation field will occur on a time scale too short for the inertial polarisation of the medium to relax. Accordingly the long wave limit of the photo-effect is determined by

$$h\nu = -E.$$

The medium polarisation energy is dissipated as heat at a later time. Thermal destruction of the polaron is accompanied by depolarisation of the medium, and the energy of heat dissociation is accordingly $-\frac{1}{3}E$ since the potential energy of the electron is 4/3 E.

The electronic polarisation does not contribute to the binding energy of the surplus electron. This treatment is equivalent to the adiabatic approximation.

(iii) The Range of Validity of the Polaron Theory.

The separation of the polarisation into two components certainly requires some justification, and may be examined in the following way.[3]

If the field produced at an ion by vibration of the electron is of the form $E_o + E_1 \cos \omega t$, the polarisation is proportional to

$$1/(\omega_r + \omega) + 1/(\omega_r - \omega) \tag{7}$$

where $\omega = E/\hbar$ is of the frequency of the polarising field, $\hbar\omega_r$ is the separation of the ground and excited states of the ion. E_o stems from the average electron distribution. If the strongly bound medium electrons have frequencies $\omega_r \gg \omega$, the electronic polarisation may respond instantaneously to the motion of the surplus electron. On the other hand, the inertial polarisation may respond only to frequencies

of the order of ionic vibrations, $\omega_r \sim 10^{13} sec^{-1}$. When $\omega \gg \omega_r$, the ions see only the average field E_o.

It therefore follows that 'such a strict subdivision of the polarisation into inertial and non-inertial components can only be achieved if the natural frequency of the electron E/h lies in the crystal transparency zone.'[2]

If the polaron model is to be a reasonable model for the surplus electron in polar liquids and crystals, the binding energy must lie between the two limits defined by the characteristic frequencies of the medium electronic and vibrational motions. Electrons in polar liquids have binding energies of the order of 1-2eV so that the effects of medium motion are unimportant. However this energy is not very different from the excitation and binding energies of the medium electrons so that electronic polarisation becomes an important feature. This behaviour contrasts with that in ionic crystals eg. NaCl, where the binding energy of the electron is small $\sim$ 0.1eV.[3] In this case the effects of lattice vibration are significant.

Uncertainty principle arguments show that medium electrons within a distance $d \sim (\hbar/\omega_r m^*)$ cannot respond instantaneously to the excess electron's motion regardless of how high their frequency ω_r becomes.[4] The electronic polarisation is then of the order of $-(1/2d)(1-1/D_{op})$. When ω_r is $\sim 3 \times 10^{15}$ sec^{-1}, d equals 0.55Å. This distance is much smaller than the circumference of the polaron orbit so that any corrections to the energy of the polaron are small.[4] Analogous statements may be made concerning the other contributions to the polarisation.

A prerequisite of polaron theory is that the electron be dispersed over a large number of centres in the medium. The displacement $\underline{D}$ is assumed to vary slowly over the lattice distance a, so that the polarisation of any ion is proportional to $\underline{D}$ and is independent of the polarisation of neighbouring sites. To justify this assumption, the polaron radius r_p must be much greater than a. To an order of magnitude, r_p is equal to the radius of the spherical region within which one half the interaction of the charge cloud and the inertial polarisation is attained, namely

$$r_p = 10/m^*C. \qquad (8)$$

Pekar's initial concepts have taken their place in the theory of solvated electrons. Long range polarisation interactions are still viewed to be an important feature of excess electron states in liquids.

B. The Importance of Cavity Formation.

As an alternative to proposing some trapping mechanism Ogg drew on experimental data to present a model for surplus electrons in ammonia.[5] Acknowledging the large volume expansion which occurs on solution of alkali metals in liquid ammonia, Ogg suggested that spherical cavities were formed in liquid, within which the electron resides.

An electron localised in such a cavity of radius R in a medium of dielectric constant D_{st} acquires a potential energy given by the Born expression

$$V = - 1/2R \ (1 - 1/D_{st}).$$

Neglecting all surface forces, collapse of the cavity is countered by a simple quantum mechanical effect, namely ' the magnitude of the de Broglie wave length of the electron must correspond to the cavity diameter leading to a zero-point kinetic energy.' Thus,

$$\lambda = 2R = h/mv$$

$$T = \pi^2 \ / \ 2R^2 \qquad \text{a.u.}$$

where T is the kinetic energy. The total energy of the electron so confined, $1/D_{st} \ll 1$,

$$E = \pi^2 / 2R^2 - 1/2R \qquad \text{a.u.}$$

is minimised when $R = 2\pi^2$ a.u. and $E = -1/8\pi^2$. The inclusion of the interactions of the electron with a positive ionic atmosphere leads to further stabilisation.

The formation of large cavities of radius 10Å is physically unrealistic, while the binding energy, -0.35eV, is low suggesting that the electronic transition is between a bound and an unbound state. Elaboration of the model is possible, but its importance lies in the contrast presented to the polaron model of Pekar. This simple cavity model emphasised that a localised surplus electron

in a liquid of high dielectric constant should be stabilised by forming a cavity around itself.

C. Subsequent Refinements of the Pekar and Ogg Models.

Pekar and Deigen[6] and Davydov[7] considered the polaron model to be applicable to the surplus electron in liquid ammonia. If the observed absorption band arises from an electronic transition between 1s and 2p states, the absorption maximum is computed to be at an energy

$$E_{max} = 0.071\ C^2\ m^* \quad \text{a.u.} \tag{9}$$

With E_{max} = 0.8eV, for the ammoniated electron,[8] the effective mass is ~ 1.6 and the polaron radius is 4.68Å.

Scaled to methyl alcohol, m* = 3.6, the computed excitation energies for the solvated electron follow the experimental trends for a variety of alcohols.[9] Deviations are observed for water, ethylene glycol and ammonia. To discuss the polaron nature of the hydrated electron, Weiss[10] suggested that the effective mass, from equation (9) and the observed E_{max} = 1.72eV, is more appropriately assigned a value ~ 3. The polaron radius is accordingly 3.3Å.

Kevan[11] modified Pekar's treatment to account for the contribution of the electronic polarisation to the binding energy. The corrected optical dissociation energy becomes

$$E_{op} = m^* \left\{ 0.164C^2 + 0.062C(1 - 1/D_{op}) \right\} . \tag{10}$$

When the interaction of the surplus electron and the electronic polarisation is the important mode of trapping, this energy is[12]

$$E_{op} = 0.5\ m^*\ (1 - 1/D_{op})^2 . \tag{11}$$

More correctly, this equation should take the same form as equation (6) with C replaced by $(1 - 1/D_{op})$.

The inclusion of the electronic polarisation contribution does have some effect on the estimated effective mass and the polaron radius. Identifying the absorption peak of the hydrated electron with the Kevan formula (10) yields m* = 0.98 and a polaron radius of 9.8Å. The original Pekar treatment gives m* = 1.27, decreasing the polaron radius to 7.6Å.

The predictive capacity of the polaron model is limited by

the lack of knowledge about the effective mass. Equating the theoretical expressions for some property with the experimental value allows some estimate to be made. Information regarding the sphere of influence of the electron in the medium may then be obtained from the polaron radius. In essence, one is determining whether the polaron model can account for the properties of the surplus electron for a choice of solvent. By studying a spectrum of similar solvents such as the alcohols, the range of applicability of the theory may be examined.

Improvements on the Ogg model recognise the importance of surface forces at the cavity boundary. Inclusion of the effects of surface tension, electrostriction and electronic polarisation of the dielectric surrounding the cavity leads to an energy for the localised state given by [13]

$$E = -0.69/R + 4\pi R^2 S + \pi^2/2R^2 \quad \text{a.u.} \qquad (12)$$

where S is the surface tension of the cavity wall. Taking a value for S equal to the macroscopic value for a plane surface in ammonia, $S=32 ergs/cm^2$ (2.06×10^{-4} a.u.), the ammoniated electron is unbound, E = +0.13eV, at the equilibrium cavity radius of 4.8Å. A larger surface tension, $48 ergs/cm^2$, increases this energy to +0.40eV while reducing the cavity radius to 4.5Å.

Increasing the attractive potential term in equation (12) to -1.0/R leads to better accord with experiment. For $S= 32 ergs/cm^2$, E = -0.87eV and R=4.2Å. Lipscomb is led to suggest that 'some specific quantum mechanical interactions appear to be necessary in order to make the cavity stable.' However, as Stairs pointed out,[14] if the electronic wave function is allowed to penetrate into the medium so that the potential energy of the electron is

$$V = -1/2R\ (1 - 1/D_{st}) \qquad r < R$$

$$V = 0 \qquad r > R,$$

with the inclusion of a simple surface tension term, the excess electron is stable by -0.35eV at an equilibrium cavity radius of 2.9Å.

The electron in a box model has been utilised to discuss the spectral behaviour of trapped electrons in organic glasses.[15] Taking the observed absorption band to be of $s \rightarrow p$ character, the simple model predicts this transition to be at an energy

$$E_{max} = 1.04\ \pi^2/2R^2. \quad \text{a.u.} \qquad (13)$$

An appropriate cavity radius is obtained by equating this relationship to the observed absorption maximum. For a range of alcohols,[16] the radius so obtained increases with the bulk of the alcohol. From n-butyl alcohol to t-butyl alcohol the cavity increases from 2.89Å to 3.27Å. As the polarity of the alcohol increases the cavity contracts. The absorption band widths are rationalised by allowing a range of cavity radii about the optimum value obtained from equation (13).

D(i) The Fusion of the Polaron and Cavity Models.

It would be a substantial improvement on the theoretical model if the best features of the Ogg and Pekar approaches could be combined in a unified theory. This synthesis was first performed by Jortner.[17] However, the concept of a trapping potential created by inertial polarisation had already proved to be of utility in a model for charge transfer to solvent spectra of negative ions in solution.[18,19] Jortner also proposed that this idea and cavity formation were the two key features of the reformulation.

At large distances from an electron disposed round a spherical cavity at r = 0 in an infinite dielectric, the displacement $\underline{D}$ is approximately given by $-\underline{r} / r^3$. The inertial polarisation is therefore, from equation (2),

$$\underline{P}_i = - C\underline{r} /4\pi r^3.$$

The potential created by this polarisation field is

$$V(r) = \int_r^\infty (P_i / r^2)dv = C/r \qquad (14)$$

This potential is assumed to be continuous up to the cavity, radius R, and constant thereafter. Perturbations of the potential near the cavity are ignored. At small distances, the displacement is not of the simple form shown above but deviates from a Coulombic form cf. equation (1). The medium molecules may also be influenced by a charge less than the electronic charge, since the wave function may penetrate the dielectric.

Relative to the energy of an electron in the conduction band of the medium, the potential energy of the electron is

$$V(r) = -C/R \qquad r<R \tag{15}$$

$$V(r) = -C/r \qquad r>R$$

The ground state wave function is represented by the 1s hydrogenic form

$$_{1s} = (p^3/\pi)^{\frac{1}{2}} \exp(-pr) \tag{16}$$

At a selected cavity radius, the optimum exponent for this function is found by minimising the energy

$$W_{1s} = p^2/2 - C/R + C \exp(-2pR)\ (pR + 1)/R \ .$$

The exponent q of the 2p excited state function

$$_{2p} = (q^5/\pi)^{\frac{1}{2}}\ r \exp(-qr) \cos\theta \ ,$$

is obtained by minimising

$$W_{2p} = q^2/2 - C/R + C \exp(-2qR)\ (1 + \tfrac{3}{2}qR + q^2R^2 + \tfrac{1}{3}q^3R^3)/R \ .$$

Regarding the electronic transition between these two states as an adiabatic transition, the inertial polarisation and the cavity radius do not change on excitation.

The energy of these two states must be supplemented by a term accounting for the electronic polarisation energy.[18] Assuming that the electron distribution may be represented by a charged sphere of radius equal to the mean radius of the orbit, the interaction energy is given by the Born formula

$$S_i = -1/2\bar{r}_i\ (1 - 1/D_{op}) \ .$$

The total electronic energy of each level,

$$E_i = W_i + S_i \qquad i = 1s \text{ or } 2p,$$

may then be used to calculate the absorption maximum for a chosen cavity radius

$$E_{max} = E_{2p} - E_{1s} \ .$$

R may be determined by matching the computed and observed absorption maxima, and the model applied to calculate some other properties of the solvated electron. Alternatively, the cavity radius may be estimated from dilation measurements, and the degree of agreement between the computed and the observed peak positions used to gauge the applicability of the model for the surplus electron in a particular solvent.

For the ammoniated electron, C = 0.523, the absorption maxima at cavity radii of 3.0Å and 3.45Å are calculated to be 0.85eV and 0.74eV respectively. At R = 3.2Å, suggested by volume expansion measurements, the computed and observed values are matched. The mean radii of the ground and excited state orbits at this cavity radius are 4.3Å and 6.6Å respectively. The electron is by no means localised within the cavity.

For the solvated electron in the lower alcohols, the predicted cavity radii are found to fall smoothly with increasing polarity except for n-butanol.[20] In methanol, D_{st} = 32.6, the cavity radius is 1.15Å, whilst in ethanol, D_{st} = 24.4, R = 1.32Å. The hydrated electron does not fit into this pattern. With a dielectric constant of ~ 80 the observed and computed excitation energies are matched at R = 1.5Å.[21-23]

The heat of solution of the excess electron may be obtained when the magnitudes of the medium polarisation energy and the energy of an electron in the conduction band of the liquid are known. Cohen and Thompson indicate that the latter quantity is small for ammonia. The medium polarisation energy, Π, for ammonia,

$$\Pi = -\tfrac{1}{2} \int_R^\infty |\psi_{1s}|^2 \, V(r) \, dv,$$

contributes some 0.475eV, when R = 3.2Å, towards the heat of solution $H = -E_{1s} - \Pi = 1.6$eV. The experimental estimate is 1.7eV.[17]

If the cavity contracts when pressure is applied, the spectrum should shift to the blue, a result qualitatively in accord with experiment. Spectral variations with temperature may be accomodated within the model by variations in each of the 1s and 2p energy levels. For the ammoniated electron

$$dE_{1s} / dT = -4.00 \, (dC/dT) + 0.409 \, (dR/dT)$$

$$dE_{2p} / dT = -3.12 \, (dC/dT) + 0.132 \, (dR/dT).$$

With a thermal expansion coefficient, $dR/dT = 3 \times 10^{-3}$ Å/°K, the shift in peak position is calculated to be in agreement with experiment.

A potential well of the form (15) can support an infinite number of bound energy levels. Since the excited state orbitals become more diffuse as the principal quantum number n increases, their energy is approximately given by

$$E_n = -C^2/2n^2 - 1/2\tilde{r}_n\ (1 - 1/D_{op}) \quad \text{a.u.} \qquad n > 2 \tag{18}$$

The asymmetry of the absorption band on the high energy side may be the result of overlapping absorption bands arising from transitions between the ground state and these higher energy levels.[17]

To distinguish this approach from those of Ogg and Pekar this model has recently been named 'the polarised cavity model'.[24]

The assumption that inertial polarisation provides the potential well for the electron entails that the medium molecules are capable of reorientation in the field of the electron. If the relaxation times are long, as in a low temperature glass or a crystal, the build-up of orientational polarisation is slow. The observation that the trapped electron in ice[25] is stable suggests that by applying Jortner's model, which relies on long-range interactions to contribute to the stability of the electron, the trapping site must be identified with a defect in the medium or that some frozen-in polarisation exists.[22]

Hamlet and Kevan conclude that the excited state of the trapped electron in aqueous glasses is unbound.[26] This is confirmed by the recent observation of a photocurrent.[27] An easy rationalisation is effected if only short-range interactions contribute to the stability of the excess electron (Section E). If it is the case that microscopic relaxation processes proceed much faster than macroscopic relaxation times[28,29] the application of the polarised cavity model may be justified.

Taking cognizance of the observations discussed in Section A(iii), concerning the subdivision of the total polarisation, for electrons in polar solvents a self-consistent field approach in which both polarisation fields are simultaneously accounted for should be adopted.[30,31]

At the limit of zero cavity radius Jortner so computes the heat of solvation of the surplus electron to be

$$E = -0.0488\ (1 - 1/D_{st})^2 \quad \text{a.u.}$$

The observed hydration energy for the localised electron in water, 1.7eV, is only approached by this formula. Although unaware of the fact, Pekar[2] also solved this problem utilising the more flexible

variational function (5), deriving the solvation energy

$$E = -0.0547\ (1-1/D_{st})^2 \quad \text{a.u.} \qquad (19)$$

From the early investigations [6,7] the absorption maximum should lie at an energy

$$E_{max} = 0.071\ (1-1/D_{st})^2 \quad \text{a.u.}$$

The excitation energies of the hydrated and ammoniated electron are so calculated to be 1.88eV and 1.72eV respectively. The use of a more flexible function increases the calculated value for the hydrated electron to 2.18eV.[32] The disparities in the observed and calculated absorption maxima is taken to imply cavity formation.

The unsatisfactory nature of calculations which impose cavity formation is illustrated by examination of the energy surfaces for the ammoniated electron[33] (see Appendix). This diagram was drawn utilising the polarised cavity model. As a consequence of neglecting the surface forces across the cavity boundary, the lowest energy configuration lies at R = 0. within the cavity models, this parameter is necessarily ascertained by recourse to some experimental observation. A satisfactory theory should uniquely determine this parameter.

(ii) Prelude to the Semicontinuum Treatment.

The models hitherto described take no account of the molecular nature of the medium in which the electron is localised. The individual characteristics of the matrix are assumed to be adequately represented by variations in the dielectric constants. To encompass the behaviour of surplus electrons within a single formula such as equation (19) is an unlikely achievement, and some deviations have been noted. The microscopic properties of a solvent are likely to manifest themselves in a more complex fashion than the early theories would suggest.

The two important advances towards the sophistication solvated electron theory were made by O'Reilly[34] and by Iguchi.[35]

To incorporate short range interactions, O'Reilly proposed that a cavity in the medium is bounded by n point dipoles μ and quadrupoles Q, at a distance $a = R + \frac{1}{2}n^{\frac{1}{3}}$ from the centre of

the void. R is the void radius and M the molecular volume. When the solvent is ammonia, the number of molecules on the periphery, approximately given by $n = 4\pi a^2 / M^{\frac{2}{3}}$, is ~23 for R = 3.0Å and M = 43Å^3. The potential energy of the electron,

$$V = 0 \qquad r > a \qquad (20a)$$

$$V = -n/a^2 \{\langle\cos\theta\rangle - Q/a\} \qquad r < a \qquad (20b)$$

$$= -4\pi/M^{\frac{2}{3}} \{\langle\cos\theta\rangle - Q/a\}, \qquad (20c)$$

is however independent of the number of molecules.

Thermal agitation of the molecules on the boundary of the cavity disturbs the alignment of the dipole moment with the field such that the angle θ subtended by the dipole moment and the radius vector is determined by

$$\langle\cos\theta\rangle = \coth x - 1/x = L(x) \qquad (21)$$

where $x = \mu E_{loc}/kT$ and E_{loc} is the local electric field acting on a molecule.

Choosing the field to be given by the simple form

$$E_{loc} = -\bar{r} / r^3, \qquad (22)$$

the depth of the well in ammonia is 4.7eV for a = 4.75Å, μ = 1.46D and Q = 1x10^{-26}esu. As a is increased from this value to 5.5Å the absorption maximum is calculated to fall from 1.20eV to 0.90eV. By far the most dominant interaction is with the permanent dipole.

The later study by Iguchi was developed in the spirit of polaron theory.

The molecular density of the solvent is taken to vary with temperature T as $n_m = n_o / \{1 + \kappa(T-273)\}$ where n_o is the molecular density at 273°K and κ is the thermal expansion coefficient. The inertial polarisation created by the interaction of the electron with solvent layers is

$$P_i(r) = n_m \mu \langle\cos\theta\rangle.$$

If the local field has the simple form (22), in which case $\langle\cos\theta\rangle = L(\mu/kTr^2)$, the potential energy of the electron, given by

equation (14) is

$$V(r) = -n_m \mu \int_r^\infty L(\mu/kTr^2)/r^2 \, dv$$

The energy levels are obtained variationally using functions of the form (16) and (17) and equation (3a) with m* = 1. The electronic polarisation is added at a later stage.

The computed excitation energies for ethanol are 1.69eV at 300°K and 1.89eV at 180°K matching well with the observed values 1.77eV (298°K) and 2.17eV (195°K).[9] Keeping the potential V(r) constant at distances less than 4.6Å spoils this agreement.[36]

E. The Semicontinuum Treatment.

Separating the nuclear and electronic motions through the Born-Oppenheimer approximation, the energy surface for a system consisting of a surplus electron in a liquid is multidimensional. The complexity of such a problem precludes the possibility of obtaining even an approximate quantum mechanical description of the electronic states. Appeal must be made to the general features which have proved to be of importance in the simplified theories and employ them in some physically reasonable model by which the stability of excess electron states in liquids may be investigated.

Adopting this viewpoint, the total energy of the system may be partitioned into the electronic energy E_e and the medium reorganisation energy E_m resulting from the disruption of the normal liquid structure. For stability, the total energy of the localised excess electron state must be lower than the energy of an electron at the bottom of the conduction band, V_o. Theoretical studies of electrons in non-polar fluids have verified this assertion.[21]

Accepting that the formation of void volumes, short- and long-range interactions are the important features of electron localisation in polar liquids, a physically reasonable model for the solvated electron may be visualised.[37]

The localisation centre is considered to be a void surrounded by a single solvation shell of N oriented dipoles at a distance r_d from the cavity centre, embedded in a continuous dielectric medium commencing at a distance r_c. The rigid alignment of these dipoles with the electric field created by the electron is opposed by thermal agitation.

The attractive short-range interactions are applied by utilising the microscopic molecular electrostatic potential derived by O'Reilly,[34] equation (20b). Long-range polarisation interactions are introduced by way of the simple Landau potential, equation (15), for the adiabatic treatment. Alternatively the SCF potential, equation (4) with C replaced by $(1-1/D_{st})$, may be used.[38]

Neglecting the quadrupole terms, the short-range attractive potential energy of the electron, given by equation (20b), is

$$V_s(r) = -(N\mu_o / r_d^2)\langle\cos\theta\rangle - N\alpha G_i^2 / 2r_d^4 \qquad (23)$$

where α is the molecular polariseability of the solvent. The local field at a molecule in the coordination shell is

$$E_{loc} = -G_i / r_d^2 \qquad (24)$$

where G_i is the total charge contained in the void volume,

$$G_i = \int_0^R |\psi_i|^2 \, dv. \qquad (25)$$

The treatment of Copeland *et al*, conducted within the adiabatic approximation, accounts for the second term in equation (23) within the electronic polarisation, while Fueki *et al* consider the inertial and electronic polarisation simultaneously. The averaging term $\langle\cos\theta\rangle$ is calculated using equations (21) and (24).

It is implicitly assumed in equation (23) that the coordination shell consists of point dipoles which can be oriented by the electric field produced by the electron at the dipole. This assumption restricts the semicontinuum treatment to solvents of small and fairly rigid molecules.

Utilising the Landau potential (15) the potential energy of the electron is therefore given by

$$V(r) = -N\mu\langle\cos\theta\rangle/r_d^2 - C/r_c \qquad r<R$$

$$V(r) = -C/r + V_o \qquad r>R.$$

Penetration of the electron into the medium is resisted by exclusion of the electron from the region occupied by the medium electrons. Such short range interactions are absorbed in the parameter V_o.

Choosing a variational wave function of the form (16),

the optimum energy is found by minimising

$$W_{ls} = p^2/2 - \left\{ N\mu\langle\cos\theta\rangle / r_d^2 + C/r_c \right\} G_{ls} - C\int_R^\infty \psi_{ls}^2 / r \, dv + (1 - G_{ls}) V_o$$

and adding the electronic polarisation energy

$$S_i = - N\alpha G_i^2 / 2r_d^4 - \tfrac{1}{2}(1 - 1/D_{op}) \int_R^\infty \left(\int_0^r \psi_i^2 \, dv \right)^2 r^{-2} \, dr.$$

The orientation of the permanent dipole depends on the wave function giving rise to a self consistent field problem.

The magnitude of V_o is not known for polar liquids, although the experimental heats of solution show that $V_o > -1.7$eV for water and $> -1.7 \pm 0.7$ for ammonia. Fortunately the depth of the potential well does not critically depend on V_o due to a balance of terms in the potential. As V_o increases, the cavity radius is likely to increase and charge will flow from the medium into the cavity. The subsequent increase in G_{is} then lowers the potential energy.

The process of cavity formation requires the investment of energy. The reorientation of the molecules on the boundary enhances both dipole - dipole and, in ammonia for example, hydrogen - hydrogen repulsions. For water, the latter term is ignored; rotation of the molecule can alleviate this interaction. Expansion of the cavity is opposed by a surface tension force $4\pi R^2 S$, the surface tension being taken as the macroscopic value, and at high pressures the work done in creating a void volume. Disruption of hydrogen bonds is neglected since the detailed structure of the solvated electron is unknown.

The medium reorganisation energy is therefore computed as the energy required to polarise the dielectric and form the cavity.

Calculation of the total energy at various void radii allows a unique determination of the cavity radius in ammonia and water. For N = 4 and 6, assuming $V_o = 0$, at 300°K the most energetically favourable centre to dipole distances are 2.72Å and 3.25Å respectively for ammonia[37] and 2.07Å and 2.58Å respectively for water.[38] An increase in V_o expands the cavity. The energies of the most stable cavities for N = 4 and 6 do not

greatly differ, indicating that some equilibrium between these two coordination numbers may exist.

The volume expansion within the semi-continuum treatment is

$$\Delta V = 4\pi/3\ (r_c^3 - N\ r_{eff}^3)$$

where r_{eff} is the effective radius of the volume occupied by each solvent molecule in the normal liquid, so that dilation measurements are interpreted as a manifestation of cavity formation and a decrease in the density of the solvation sheath over the normal liquid. For ammonia, N = 4 and r_c = 4.22Å, the volume increment is 66.8 ml/mole, matching quite well Schindewolf *et al*'s experimental measurement 84 ± 15 ml/mole at 240°K.

The vertically excited state electronic energy is

$$E_{2p} = q^2/2 - G_{2p}\left\{N\mu\langle\cos\theta\rangle/r_d^2 - C/r_c\right\} - C\int_R^\infty \psi_{2p}^{\ 2}/r\ dv$$
$$+ (1 - G_{2p})V_o + S_{2p},$$

with $\langle\cos\theta\rangle$ appropriate to the ground state.

In general, the excitation energies are overestimated but of the correct order of magnitude. Further, the inclusion of long range polarisation appears to be necessary to lower the energy of the excited state.[29,40]

Experimentally, Kawabata[41] finds the excited state in ice to be bound. Theory predicts the vertical 2p state to be unbound, but no autoionisation to the conduction band takes place, whereas the relaxed excited state in water and ice exhibits no energy minimum.

The best understood energy level structure from photo-bleaching phenomena is for trapped electrons in 2-methyltetrahydrofuran glasses.[40] Excitations to the unrelaxed excited state and the conduction band or an autoionising state occur at energies ~1.0eV and 1.6 ± 0.2eV respectively. Relaxation of the excited state results in crossing to a relaxed 2s state some 1.1eV below the relaxed conduction band.

Theoretical calculations support this picture.[42] For n = 4 and V_o = -0.5 the 1s→2p transition is calculated at 1.0eV while the transition to the unrelaxed conduction band is placed at 1.4eV. The relaxed 2s state lies 0.1eV above the relaxed 2p state along the configurational co-ordinate and crosses near its minimum. Excitation from this state to the relaxed conduction state is placed at 0.6eV in

fair agreement with 1.1eV from experiment.

Some calculated properties for the ammoniated and hydrated electrons are compared with observation in Table 1.

Table 1.

Experimental and calculated properties for the solvated electron. $n = 4$, $V_o = 0$.

	Ammonia (203°K)		Water (300°K)	
	Obs.	Calc.[37]	Obs.	Calc.[38]
E_{max} (eV)	0.80 (240°K)	1.19	1.72	2.11
Half-linewidth(eV)	0.46	0.12	0.92	0.18
Oscillator strength	0.77	0.49	0.71	0.78
ΔH (eV)	1.7 0.7	1.43	1.7	1.94
ΔV ml/mole	84 ± 15	66.8	1-6	25

Exact agreement with experiment would be fortuitous but overall the semicontinuum model reproduces many of the observed features quite well. Some discrepancies remain, in particular concerning the band width.

The semicontinuum treatment presents a great advance in the theory over the early models. However, some criticisms may be made.

The medium rearrangement energy is introduced in a coarse fashion. For example, it is open to debate as to whether a macroscopic surface tension force exists at molecular dimensions. The acceptance of such forces entails that cavities are created in the medium by the electron. When the localisation site exists naturally, no such surface tension force is operative.

The model permits one configurational coordinate, the void radius R, so that the cavity can only 'breathe' symmetrically, while other modes are possible.

Although the forces determining the structure of the second solvation shell are not pure charge-dipole interactions, the substantial penetration of the electronic wave function into the medium serves to illustrate that effects in this layer may be important.

In completing this review of solvated electron theory, it may be noted that the viewpoint taken of the surplus electron has

subtely changed on proposal of the semicontinuum model. The polaron treatment considers electron trapping by polarisation fields while the current conception resembles that of a solvated ion around which solvent dipoles have been oriented. Referring to the suggestion of Weiss that the trapped electron in water be called a 'polaron' and not a 'hydrated electron',[10] it may indeed now be permissable to speak of the 'hydrated electron'.

References to Chapter 3.

1. L. Landau, Sov. Phys., 3, 664 (1933).
2. S. Fekar, J. Phys.,(USSR), 10, 341,347 (1946).
3. J.J. Markham, Solid State Physics, 8, 312 (1966).
4. R.A. Marcus, J.Chem.Phys., 43, 3477 (1965).
5. R.A. Ogg, Phys.Rev. 69, 669 (1946).
6. S.Pekar and M.F. Deigen, Zh.Eksp.Teor.Fiz., 18, 481 (1948).
7. A.C. Davydov, Zh.Eksp.Teor.Fiz., 18, 913 (1948).
8. R.K. Quinn and J.J. Lagowski, J.Phys.Chem., 73, 2326 (1969).
9. M.C. Sauer, S. Arai and L.M. Dorfman, J.Chem.Phys., 42, 708 (1965).
10. J.J. Weiss, Nature, 199, 589 (1963).
11. L. Kevan, Prog.Solid State Chem., 2, 304 (1965).
12. P.N. Moorthy and J. Shankar, Rad.Eff. 2, 91 (1969).
13. W.N. Lipscomb, J.Chem.Phys., 21, 1429 (1953).
14. R.A. Stairs, J.Chem.Phys., 27, 1431 (1957).
15. M.J. Blandamer, R. Catterall, L.Shields and M.C.R. Symons, J.Chem.Soc., 4357 (1964); M.J. Blandamer, L. Shields and M.C.R. Symons, J.Chem.Soc., 1127,3759 (1965).
16. A. Ekstrom and J.E. Willard, J.Phys.Chem., 72, 4599 (1968).
17. J. Jortner, J.Chem.Phys., 30, 839 (1959).
18. R. Platzman and J. Franck, Z.Phys., 138, 411 (1954).
19. G. Stein and A. Treinin, Trans.Farad.Soc., 55, 1086,1091 (1959).
20. S.Noda, K. Fueki, Z. Kuri, Bull.Chem.Soc.Japan, 42, 16 (1969).
21. J. Jortner, Actions chimiques et biologiques des radiations, ed M. Haissinsky, p7.
22. P.S. Julienne and L.P. Gary, Mol.Cryst., 5, 135 (1968).
23. J. Jortner, Proc.Colloq.Weyl II, ed J.J. Lagewski and M.J. Sienko, p49., Butterworths, London (1970).
24. B.C. Webster and G. Howat, Rad.Rev. (in press).
25. I.A. Taub and K. Eiben, J.Chem.Phys., 49, 2499 (1968).
26. P. Hamlet and L. Kevan, J.Amer.Chem.Soc., 93, 1102 (1971).
27. I. Eisele, R. Lapple and L. Kevan, J.Amer.Chem.Soc., 91, 6504 (1969); I. Eisele and L. Kevan, J.Chem.Phys., 53, 1867 (1970).
28. N.E. Hill, W.E. Vaughan, A.H. Price and M. Davies, in Dielectric Properties and Molecular Behaviour, p298, Van Nostrand, London (1969).
29. G. Nilsson, J.Chem.Phys., 56, 3427 (1972).
30. J. Jortner, Mol.Phys., 5, 257 (1962).
31. J. Jortner, Rad.Res.Suppl., 4, 24 (1964).

32. K. Fueki, D.F. Feng and L. Kevan, Chem.Phys.Lett., 4 313 (1969).
33. G. Howat and B.C. Webster, Ber. Bunsenges. Phys. Chem., 75, 626 (1971).
34. D.E. O'Reilly, J.Chem.Phys., 41, 3736 (1964).
35. K. Iguchi, J.Chem.Phys., 48, 1735 (1968).
36. K. Iguchi, J.Chem.Phys., 51, 3137 (1969).
37. D.A. Copeland, N.R. Kestner and J. Jortner, J.Chem.Phys., 53, 1189 (1970).
38. K. Fueki, D.F. Feng and L. Kevan, J.Phys.Chem., 74, 1976 (1970); K. Fueki, D.F. Feng, L. Kevan and R.E.Christoffersen, J.Phys.Chem., 75, 2297 (1971).
39. U. Schindewolf, R. Vogelsgesang and K.W. Boddeker, Angew.Chem.Int.Ed.Engl., 6, 1076 (1967).
40. T. Huang, I. Eisele, D.P. Lin and L. Kevan, J.Chem.Phys., 56, 4702 (1972).
41. K. Kawabata, J.Chem.Phys., 55, 3672 (1971).
42. K. Fueki, D.F. Feng and L. Kevan, unpublished calculations, quoted in ref. 40.

CHAPTER 4.

THE MOLECULAR APPROACH.

A(i) Introduction.

It has been emphasised in Chapter 3, that the current theories of surplus electrons in polar liquids rely on being able to replace the surrounding medium by a dielectric continuum. Short-range medium-electron interactions are incorporated into the semi-continuum modelvia an electrostatic potential arising from point dipoles on the boundary between a cavity and the continuous dielectric medium.

However, at the localisation centre, the microscopic structure of the medium will manifest itself through a non - spherical local potential experienced by the surplus electron, so modifying its properties. Electrostatic models fail to highlight these local variations in the potential. In addition, if the excess electron is sufficiently well localised, the bulk dielectric properties of the medium will be inadequate to portray the potential experienced by the electron. Long-range polarisation interactions in this case do not dominate the properties of the surplus electron state.

The molecular approach takes the alternative viewpoint and examines the microscopic structure of the localisation site. The surplus electron is considered to be trapped at, and stabilising, a cluster constructed from a variable number of solvent molecules. The energy of the electron depends not only upon this number, but on their orientation. In time, reorganisation of such clusters will provide a variety of different sites in the liquid within which the electron resides.

The energy of these charged molecular aggregates may be investigated using molecular orbital theory. This method by-passes the need to differentiate between the medium and the surplus electrons. All interactions are simultaneously accounted for. Important features such as spin polarisation are naturally incorporated in this method. This effect cannot be studied in any other way.

The sole properties which are immediately open to investigation are those which arise mainly as a result of local interactions. Relatively distant disturbances in the medium are assumed to have a minor effect.

Dye has indicated some examples of this nature for metal-ammonia solutions[1] which may be in accord with the interpretation that they arise from local interactions. As the metal concentration in ammonia increases from dilute to moderate, the absorption band shape, extinction coefficient and electron relaxation are independent of the metal concentration while the peak position in the optical absorption spectrum is only slightly concentration dependent.

This chapter is devoted to the molecular approach. Molecular models are proposed for the hydrated and ammoniated electrons and the energy of each cluster is calculated using the semi-empirical INDO molecular orbital method.

(ii) Some Early Molecular Models for the Solvated Electron.

In the spirit of a molecular orbital treatment, Kaplan and Kittel assumed that the orbital of the ammoniated electron was a linear combination of 1s and 2p atomic orbitals centred on the hydrogen nuclei at the boundary of a cavity.[2] Although no energy calculation was performed, polarisation effects were assumed to deplete the 1s character of the molecular orbital to ~50%. This model is similar to that proposed for the F - centre in alkali halides by Kahn and Kittel.[3] The number of ammonia molecules surrounding the cavity was taken to be ~17.

This basic model has been utilised extensively in investigations pertaining to the hydrated electron.[4] A structural model comprised of four tetrahedrally disposed molecules with four protons directed towards the centre was considered. This system may be envisaged to be formed by molecular reorientation round a vacancy in the ice I lattice. Molecular orbitals are constructed from scaled 1s orbitals centred on the inner hydrogen nuclei. Coulombic interactions between the surplus electron and the tetramer nuclei and the electrons provide a potential well within which the electron resdies. Exchange interactions and perturbation of the water orbitals are neglected.

At an oxygen-oxygen distance of 2.76Å, appropriate to ice, the ground state is calculated to lie at -4.38eV and the triply degenerate excited state at -3.58eV. The optical excitation energy is so calculated to be 0.8eV, which is approximately half the observed value 1.72eV ($300^{\circ}K$)[5]. In order to match this value, Natori found

it necessary to distort the geometry of the water molecules.

Estimating the energy investment in the formation of this structure to be 2eV, the heat of hydration is 2.4eV, comparing quite well with an observed 1.7eV.

The treatment suffers from the deficiency that the total energy of the system is not open to evaluation. At least one experimental observation is required to evaluate the parameters within the model. Whether this structure is stable or not remains to be ascertained.

The first investigation of the configurational stability of a solvated electron model was undertaken by Raff and Pohl.[6] Dimeric structures were proposed to represent the immediate environment of the solvated electron in eight media.

The electron is considered to be bound in the field of two opposed molecular dipoles, written for hydrogen fluoride

$$F - H \ldots e^{-} \ldots H - F.$$

To simplify the calculation, this system may be viewed as a hydrogen molecule ion perturbed by two fluoride ions

$$F^{-} \ldots H_2^{+} \ldots F^{-}.$$

The molecular orbitals for the excess electron may then be taken to be linear combinations of screened hydrogenic 1s functions centred on the protons. The screening constant is estimated in an empirical manner.

The transition energies, $\sigma_g \rightarrow \sigma_u$, are computed to be 2.39eV and 1.63eV at equilibrium proton-proton separations of 1.67Å and 1.88Å for the hydrated and ammoniated electrons respectively. For such a crude model, the prediction of excitation energies to within approximately 90% of the observed absorption maxima is somewhat fortuitous. The importance of the treatment lies in the recognition that energetic quantities should be evaluated at equilibrium configurations and not artificially matched with observation.

The CNDO/2 studies of Weissmann and Cohen into hydrated electron models also suffer from this deficiency.[7] Within the approximations involved, the most favourable structure for the hydrated electron is reported to be a normal ice - like structure, and the excitation energy is placed at 3.8eV. Whether the single geometry studied represents a minimum energy configuration or not

is not considered. In addition, the CNDO method has been shown in Chapter 2., Section D, to be inadequate for the investigation of open-shell systems.

(iii) A Stability Criterion for the Molecular Cluster.

The localised excess electron state becomes stable when the energy of such a state is lower than that of the quasi - free electron. When the molecular approach is utilised, the cluster is essentially isolated, and any effects arising from the surrounding medium are neglected. The cluster may perhaps be viewed as persisting in the gas phase, so that some other criterion is required to determine the stability in the prescence of the surplus electron.

For a system containing n solvent molecules S and an electron, the total energy of a stable species must be lower than the energy of the separated molecules and an electron. The latter state, hereafter called the reference state, may formally be written $(n-1)S + S^-$ where the electron has been associated with one solvent molecule. For stability,

$$E_{st} = E\left[(S_n).e^-\right] - E\left[(n-1)S + S^-\right] < 0. \qquad (1)$$

This energy difference may be partitioned in a revealing way. If the electron affinity of the solvent S is

$$A(S) = E(S^-) - E(S),$$

relation (1) may be written as

$$E\left[(S_n) - nS\right] + \left[A(S_n) - A(S)\right] < 0. \qquad (2)$$

The first term in this expression is the energy required to synthesise the solvent cluster, whilst the second measures the difference in electron affinity of the cluster and an isolated molecule.

Providing the former quantity is relatively small, the cluster of molecules will stabilise the electron if the electron affinities of the solvent and complex are disparate. The electron affinity of a cluster is likely to be smaller (less positive) than the electron affinity of a solvent molecule, so that solvents of high and positive affinities may be expected to yield stable species.

Intuitively this stability criterion seems to make chemical sense.

Large positive electron affinities arise when the electron is forced to enter a highly antibonding orbital on the solvent molecule. Such orbitals generally have a large spatial extension, and electron density flows over the molecular system and is stabilised.

For future reference, the computed energies, within the INDO approximation, for neutral and negatively charged water and ammonia molecules are collected in Table 1.

Table 1.

The computed energies (a.u.) for the water and ammonia molecules and their negative ions.

H_2O	-19.2519	H_2O^-	-18.9867
NH_3	-13.5299	NH_3^-	-13.2756
NH_3 (planar)	-13.5261	NH_3^- (planar)	-13.2925

B(i) Some Dimer Models for the Solvated Electron.

As a first stage in the investigation of molecular cluster models for the hydrated and ammoniated electrons, various dimer models have been considered.

The process envisaged during solvation may be described as follows. Thermalised electrons are trapped at a dimeric site in the liquid in a time comparable with the dielectric relaxation time. Subsequent reorientation of the dimeric fragments may follow. The full trapping ability of the liquid may be further developed by the involvement of additional molecules in the trapping site.

Figure 1 depicts the geometry of three dimer models for the hydrated and ammoniated electron. Structure III is a fragment detached from the wurzite ice structure, while models I and II are planar. Structure I for the hydrated electron bears some resemblance to the 'D defect' invoked by Bjerrum in order to rationalise the dielectric relaxation phenomena observed for ice.[8]

INDO molecular orbital calculations were carried out at several intermolecular distances for each model. The angle α in the

Figure 1. The geometries for the dimer structures I, II and III for the ammoniated and hydrated electrons.

Structure I

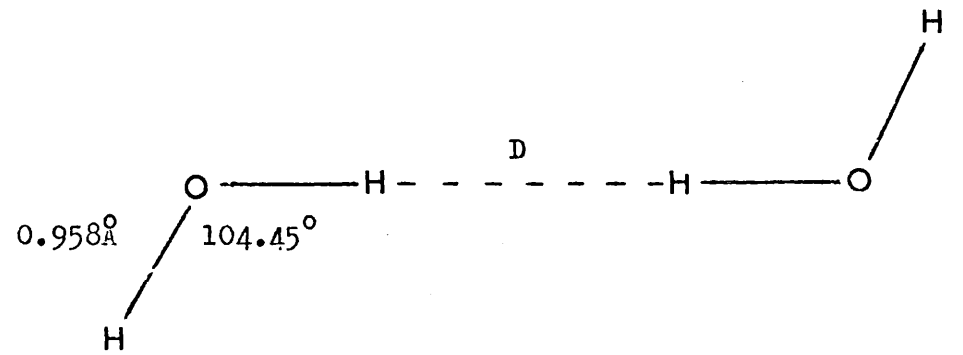

Structure II

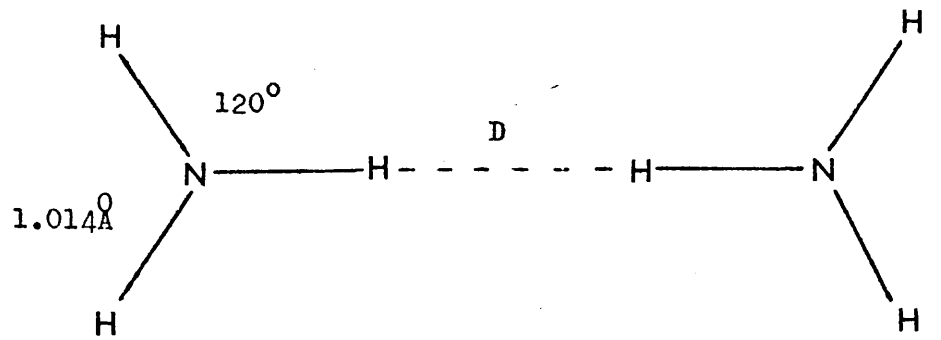

Structure III

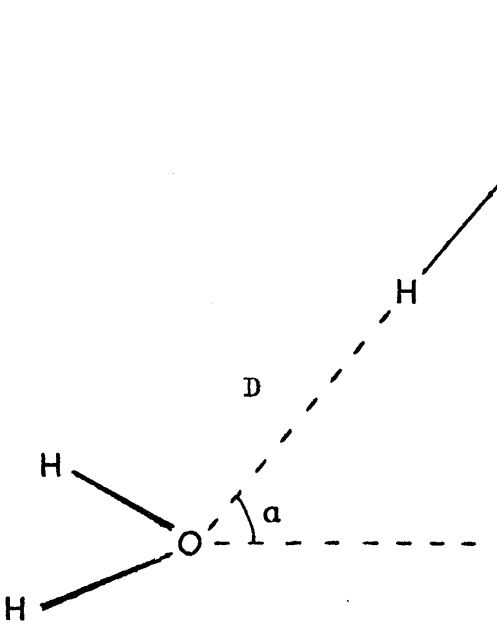

Figure 2. The total energy variations for the dimer structures I, II and III (α = 0) with intermolecular separation. The reference state energy in each diagram is highlighted by the broken line.

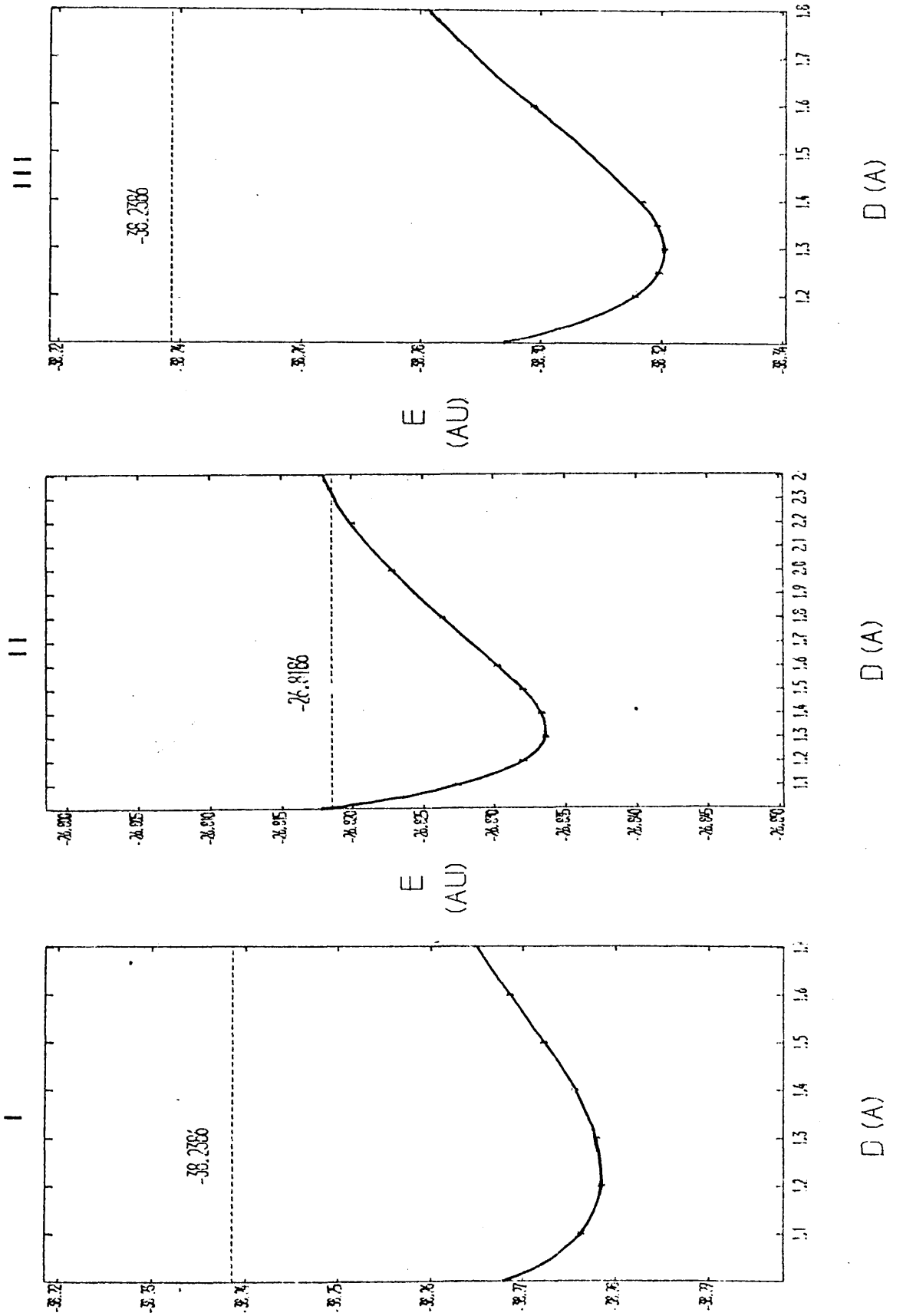

ice-like structure III was varied between 0° and 90°. The computed energies are displayed in Tables 2,3, and in Figure 2. The tables are collected together at the end of this chapter. The reference state energy for each model is highlighted in the figure.

It is immediately apparent that all the dimeric structures portray a stable equilibrium geometry in the prescence of the excess electron. The optimum intermolecular separations for structures I and II are gauged to be at 1.2Å and 1.3Å respectively. These distances are approximately 0.4Å smaller than the calculations of Raff and Pohl suggest.[6]

The study of McAloon and Webster,[9] conducted within the extended Hückel method, assigned intermolecular distances by matching the observed transition energies and the difference between the energies of the lowest unoccupied virtual orbital and the highest occupied orbital. The separations so obtained were 1.5Å for structure I and 3.52Å for structure II. This procedure has already been criticised.

The INDO calculations locate the optimum intermolecular distances for the structure III at 1.30Å for $\alpha = 0^{\circ}$ and 1.35Å for $\alpha = 90^{\circ}$ with a smooth variation between these limits.

At the most energetically favourable geometry, on utilising equation (1) and the data in Table 1, structures I - III lie 1.09eV, 0.41eV and 2.23eV ($\alpha = 0^{\circ}$) respectively below the reference state energy. The most favourable conformation for the ice-like dimer III is at $\alpha = 0^{\circ}$. The energy difference between $\alpha = 0^{\circ}$ and 90° is some 0.33eV.

The larger stabilisation energy for structure III over structure I is maintained for all intermolecular angles. Partitioning the stabilisation energy in the manner of equation (2) may illuminate this preference.

At the equilibrium geometries above, when the electron is removed, the dimers I and III have energies -38.4953 a.u. and -38.5201 a.u. ($\alpha = 0^{\circ}$) respectively. Some 0.23eV is therefore required to form structure I, whilst an energy gain 0.45eV is made on forming structure III. The electron affinities of these structures are calculated to be 5.90eV for model I and 5.43eV for model III. The ice-like structure is therefore favoured due to the larger affinity for electrons and the energy gain on forming this structure.

(ii) The Excitation Energies.

Transition energies at each intermolecular separation for structures I, II and III were evaluated by the method described in Chapter 2, Section E.

At the equilibrium geometries, the excitation energies are computed to be 1.98eV for the hydrated electron model I and 1.10eV for the ammoniated electron model II. A much higher value, 5 - 6eV, is obtained for structure III. The two former values match the experimental observations of 1.72eV for the hydrated electron and 0.80eV (240°K) for the ammoniated electron.[10]

The variation in calculated excitation energy with intermolecular geometry is shown in Tables 4 and 5.

For planar structures I and II, a decrease in the intermolecular separation shifts the transition energy towards the blue. From Table 4, a compression of the dimer intermolecular distances by 0.1Å increases the excitation energy by 0.18eV and 0.13eV for structures I and II respectively. If the effect of increased pressure on these systems is reflected in smaller intermolecular separations, the absorption maximum is predicted to shift to shorter wavelengths. This result is in qualitative agreement with experiment. Conversely, if a temperature increase expands the dimer structure, a red shift is indicated, in qualitative agreement with experiment.

If such dimeric structures are initially formed in radiolysed water and ammonia, an interesting spectral phenomenon is predicted to occur. In water at 0°C, the two nearest neighbour oxygen atoms lie at 2.83Å and 3.27Å for the ice I structure.[11] In ammonia at 199°K the nearest nitrogen atom lies at ~3.56Å.[12] If dimer structures of the types I and II are formed, the proton-proton separations are 0.91Å and 1.35Å for model I and 1.53Å for model II.

As the water dimer relaxes, the proton-proton separation may move towards ~1.2Å. The spectrum, if observed at a short enough time, will be seen to build up as two high and low energy bands coalesce. Alternatively the initial spectrum may narrow. The ammonia dimer spectrum is predicted to shift to the blue.

No such shifts have yet been detected for these systems. If the microscopic relaxation time is very short, the above processes may not be easily observed.

Figure 3. The variation in calculated excitation energy , E_{max}, with intermolecular angle for two intermolecular distances, D(Å), of structure III.

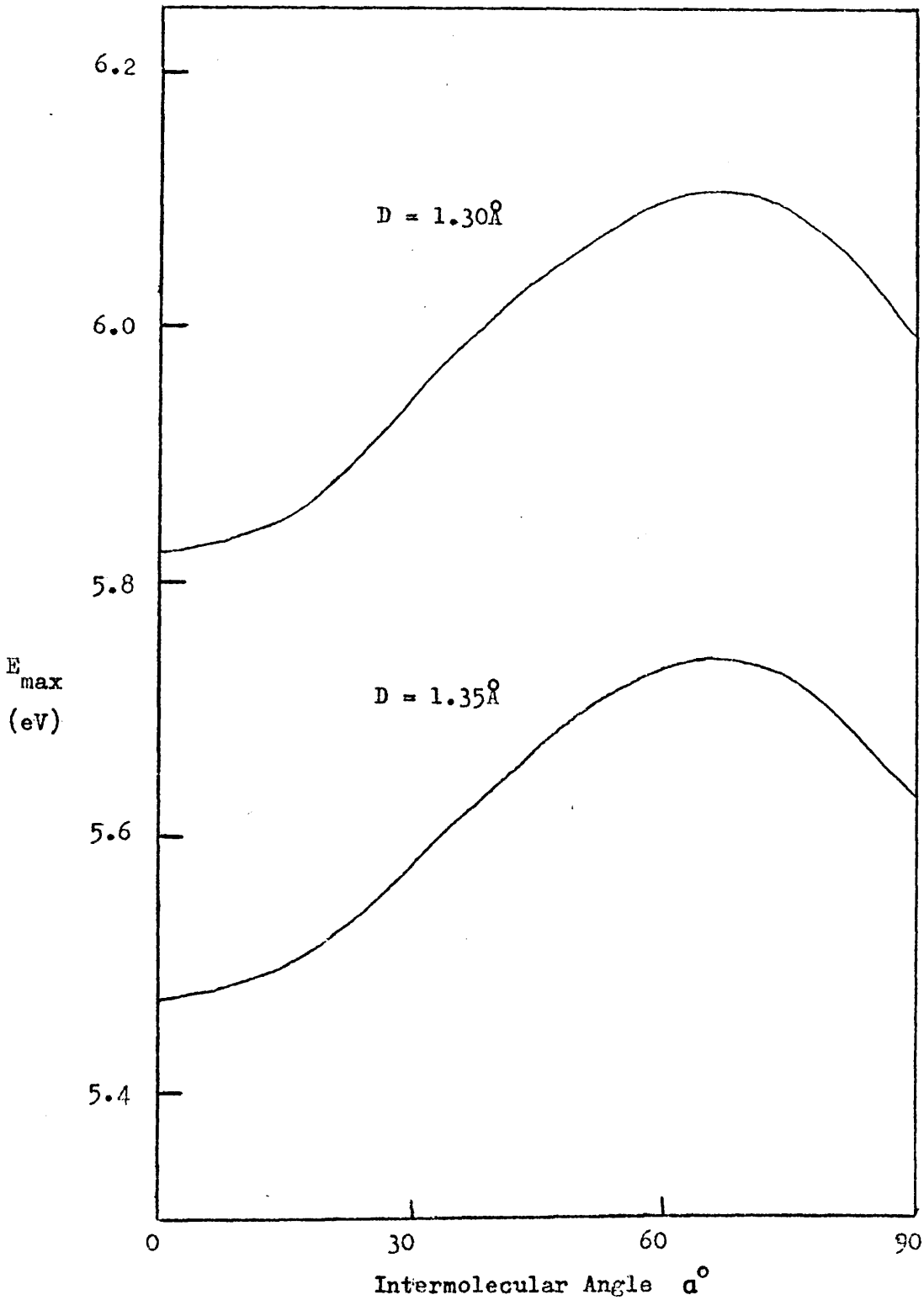

The behaviour of the excitation energy with the geometry of the ice-like fragment III is more complex.

Over all intermolecular angles, the data displayed in Table 5 shows that a compression of the intermolecular distance D, results in an increase in the excitation energy.

Although, as α varies, the excitation energy is computed to be rather large, 5 - 6ev, the interesting feature of this variation is that the excitation energy exhibits a maximum in the range $\alpha = 45^{\circ} - 70^{\circ}$. The wurzite angle in ice is $54^{\circ}44'$. If this behaviour, illustrated in Figure 3, is proved to be substantiated in the light of further studies, a rationale of some spectral phenomena may be effected.

When the cluster is initially stabilised by the trapped electron, the geometry of the site may be expected to vary. As the cluster relaxes, the intermolecular orientation might be expected to move towards angles in the central region so depleting the number of geometries at angles $\alpha = 0 - 10^{\circ}$ and $\alpha = 80 - 90^{\circ}$. The absorption spectrum, if observed before this time, will reveal a band maximum at lower energies than the final spectrum.

Bathing such a system in light of shorter wavelength than the absorption maximum may invoke a 'photo-shuttle' effect and repopulate the traps with angles away from the central region. The spectrum will shift to the red. Irradiation at longer wavelengths empty the lower energy traps and a shift to the blue in the spectrum is effected. These predictions are in accord with photobleaching experiments on irradiated alkaline glasses.[13]

Compression of the cluster results in a blue shift, expansion results in a red shift. The red shift with temperature may be further enhanced by increasing the number of orientations lying away from median angles. These conclusions are in qualitative agreement with the experimentally observed effects of pressure and temperature on the absorption maximum of the hydrated electron.

The structures I and II may also be utilised to rationalise the bleaching phenomena by making the assumption that traps of different depths exist in the liquid. Shallow traps have intermolecular distances larger than the optimum geometry.

The magnitude of the calculated excitation energy for structure III is a warning against a too ready acceptance of the

description of bleaching phenomena using this model. It is not intended that too much emphasis be placed on the behaviour for this cluster until further studies of larger clusters are performed at a more accurate level of calculation.

An examination of the charge distributions for the dimer models indicates a possible source of an excitation energy of this magnitude.

(iii) The Charge Distributions for the Dimer Models.

The computed charge densities of the excess electron at each atom for Structures I - III are displayed in Figures 4 and 5. Figure 4 portrays the ground state distribution, and Figure 5, the excited state distribution. The charge densities calculated by McAloon and Webster[9] by performing a population analysis on the extended Hückel molecular orbitals are included for comparison in Figure 4.

The INDO calculations reveal that in the ground state, the surplus electron is delocalised overthe molecular framework of the water and ammonia dimers I and II. There is also to be noted a slight preference for the electron to reside on the protons near the centre of the dimer. The major portion of the charge lies on the hetero-atoms.

This distribution is in direct contrast to that obtained from the extended Hückel calculations. Within this approximation, the dimeric protons retain most of the charge. Delocalisation takes place only in the water structures I and III. The contrast displayed in the charge densities for these two dimers, I and II, was invoked to rationalise the observation that the polaron model appears to be a better theoretical model for the hydrated electron than for the ammoniated electron, as noted in Chapter 3, Section D(i). This conclusion no longer obtains. The INDO studies conclude that delocalisation is appreciable in both solvents.

An examination of Figure 5 shows that on excitation the charge is dispersed towards the outer regions of the structures I and II.

In the ground state, the charge on model III is almost completely localised on one molecule. This disposition is maintained for all orientations. When excitation occurs, the

Figure 4. The ground state charge distributions of the surplus electron computed by the INDO (right hand side) and the extended Hückel methods (left hand side)[9] for the dimer structures I, II and III.

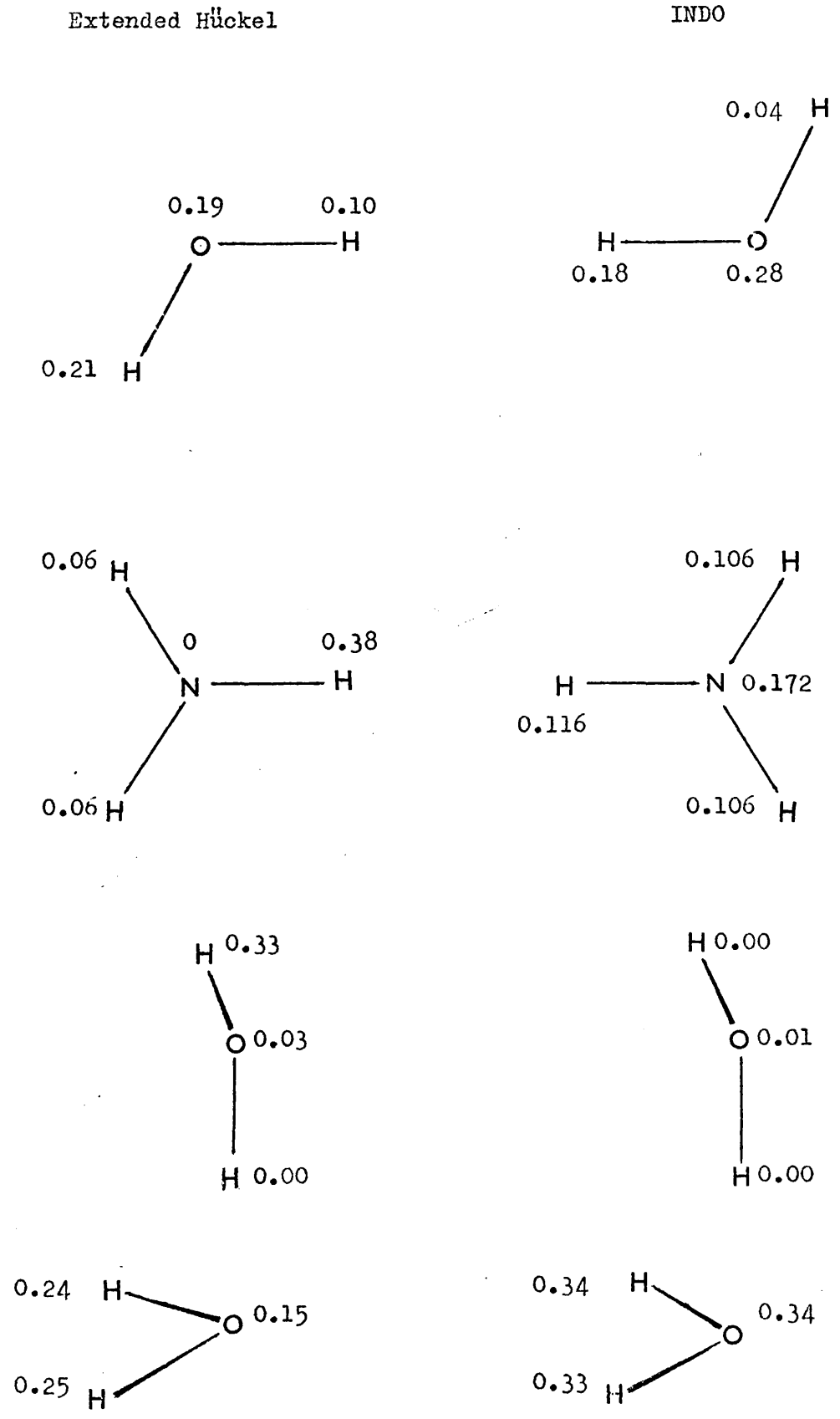

Figure 5. The excited state charge distributions of the surplus electron computed by the INDO method for the dimerstructures I, II and III.

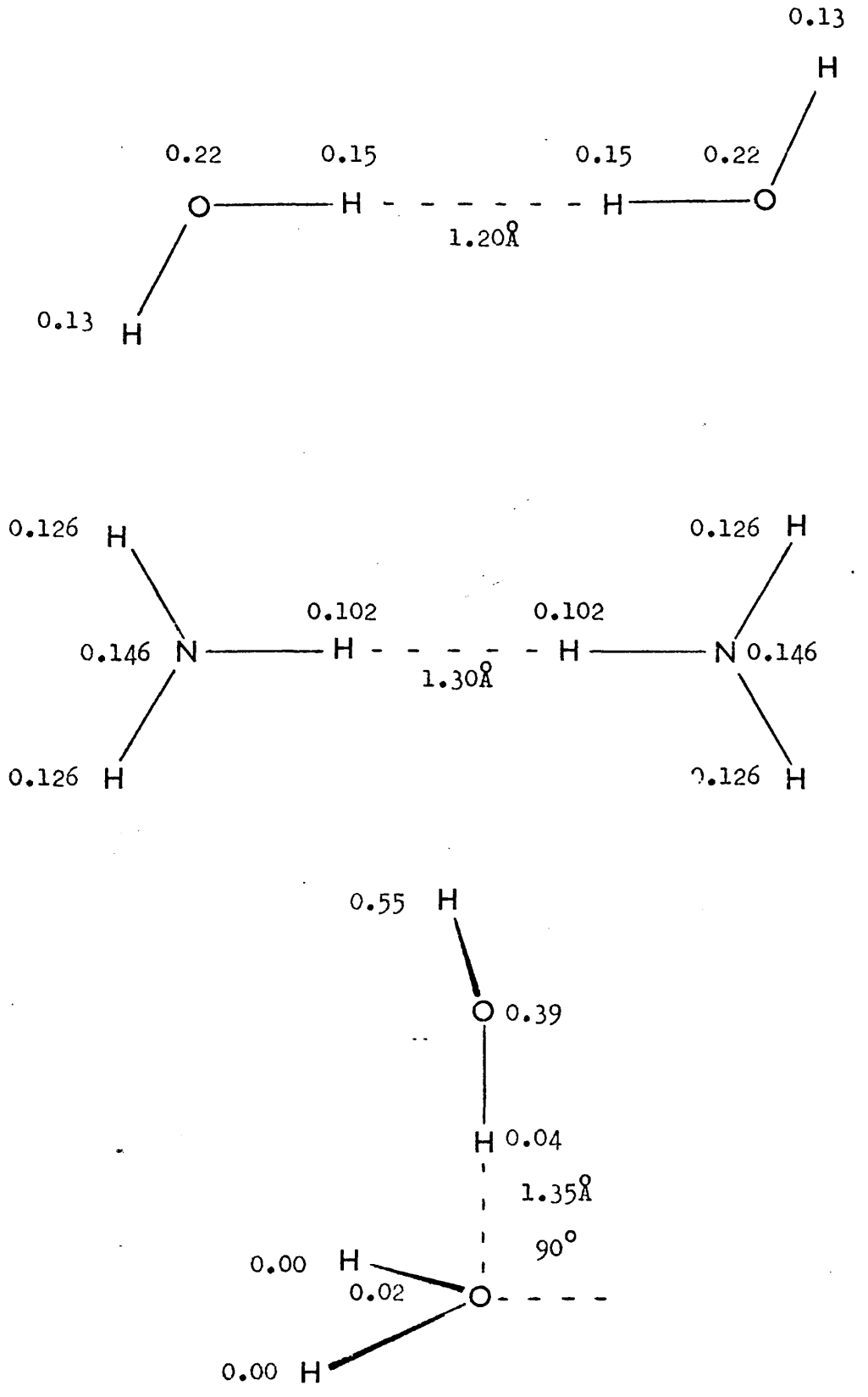

charge is seen to 'hop' from one molecule to the other. Herein may lie the reason for the large excitation energy computed for this structure.

It was asserted in Chapter 2, Section E, that when charge redistribution on excitation is significant it may be necessary to employ configuration interaction techniques or to perform a new SCF calculation for the excited state. The ice-like structure III does indeed exhibit extensive charge movement.

On de-excitation, the electron may be stabilised on a site other than the original molecular cluster. This movement of charge is reminiscent of a photocurrent. Recently, reports of photoconductivity in γ-irradiated alkaline glasses have been made,[14] although such behaviour has not been observed in water.

(iv) Some Alternative Dimer Models.

In Figure 6, four dimer models are depicted. The dipole moments of the constituent molecules are directed towards the centre of the cluster. In structures IV and VI the intermolecular proton-proton distances are minimised. This interaction is minimised in structures V and VII by rotation about the symmetry axis running through the two hetero-atoms in each model.

At a choice of intermolecular distances, Table 6 shows the computed total energies. It can be seen that each dimer structure attains an equilibrium geometry.

When the lowest computed energy is compared with the reference state energy none of these structures, excepting V is predicted to be stable. The stability of dimer V over the reference state is a mere 0.005eV, far less than any of the structures I - III. The utility of these dimer models is therefore low, and will not be further discussed.

(v) The Dimer Model Calculations in Perspective.

It would be imprudent to entertain the conception that a dimer model represents the structure of the solvated electron. Indeed it is highly unlikely that this species may be fully understood on the basis of such structures. As an example of the degree of complexity which may be involved in taking the molecular approach, recent magnetic resonance studies of metal-ammonia solutions detect

Figure 6. The geometries of the dimer models IV, V, VI and VII for the ammoniated and hydrated electrons.

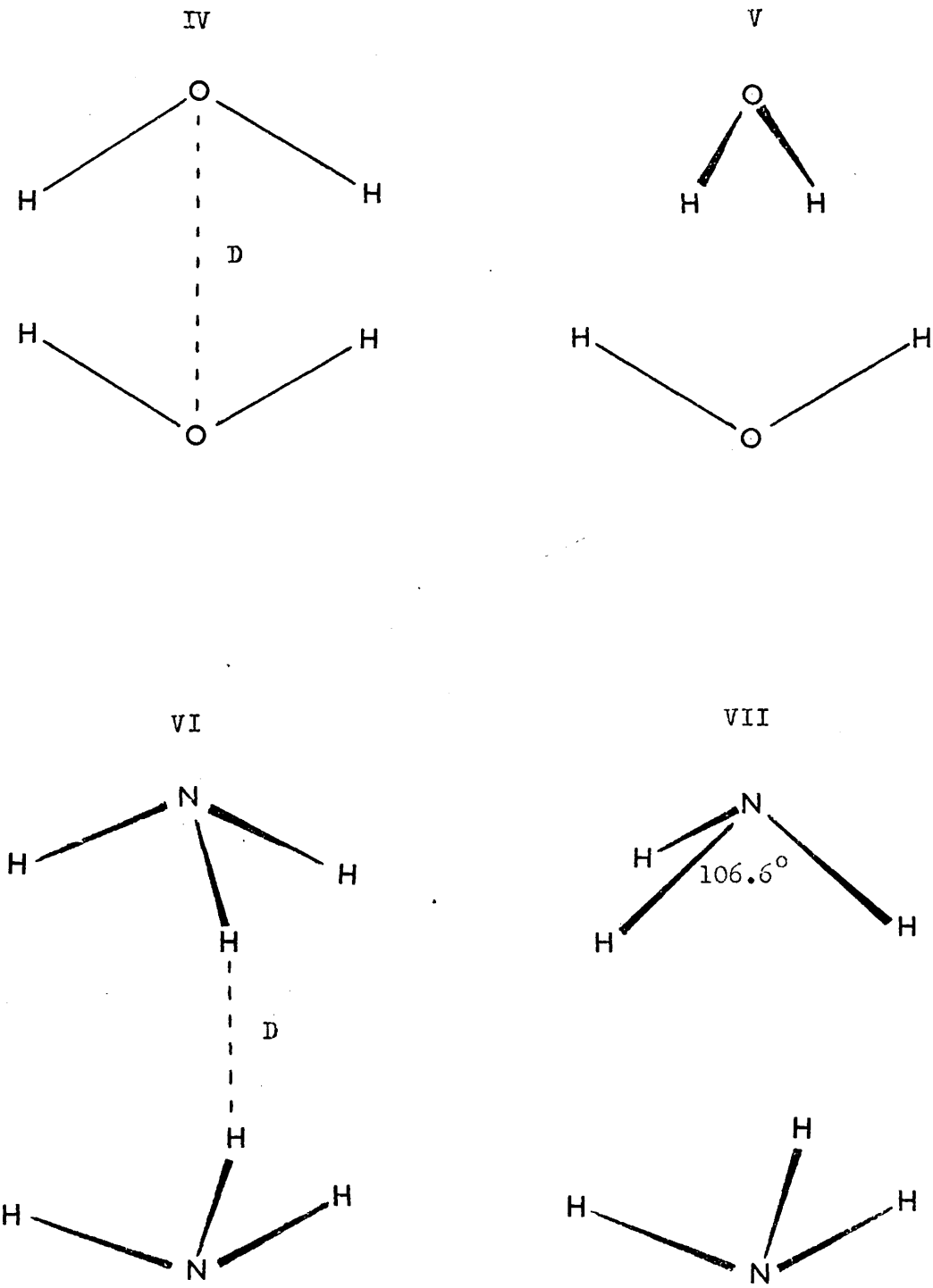

the interactions of the surplus electron with some 3 - 13 ammonia molecules.[15] However, it is hoped that some of the important features of the solvated electron may be recognised within a simple model such as the dimer structures. Further, as previously discussed, the existance of dimeric sites in the liquid may be important in the processes leading to stabilisation of the localised electron state.

The main features which have been distilled from the dimer model calculations may be summarised as follows.

With changes in the molecular geometries of the dimer models, predicted variations in spectral phenomena appear to be in qualitative accord with experimental observations. Some measure of success, perhaps fortuitous, has been achieved in the calculations on structures I and II for which the match of calculated and observed excitation energies is fair.

The electronic distribution of models I and II highlights the tendency of the excess electron to be delocalised but with a preference to lie on protons near the cluster centre. Dispersal of charge occurs on excitation.

The ice - like dimer calculations allow some speculations to be made concerning the spectral changes as the cluster relaxes. A mechanism for electron migration is indicated.

Attention is now directed towards the investigation of some tetramer models for the solvated electron in water, ammonia and water-ammonia mixtures. These structures may be a more physically reasonable representation of the localisation site than the dimer structures.

C(i) Some Tetramer Models for the Hydrated and Ammoniated Electrons.

A defect tetramer model for the hydrated electron which has been the focus of a great deal of theoretical interest is illustrated in Figure 7, and labelled VIII. This structure may be formed by the removal of a tetrahedrally coordinated water molecule in the wurzite ice-lattice followed by reorientation of the four remaining molecules such that four protons point towards the tetrahedron centre.

This model is found to be compatible with many experimental observations concerning the surplus electron in aqueous media. The similarity in the spectra, E_{max} = 1.72eV (300°K) in water,[5] 1.94eV (77°K) in crystalline ice[17,18] and 2.12eV (77°K) in alkaline ice,[19] in conjunction with the lack of any sharp discontinuity at the

Figure 7. The tetramer structures for the hydrated and ammoniated electrons. D is the distance from the centre of the tetrahedron to the vertices.

VIII

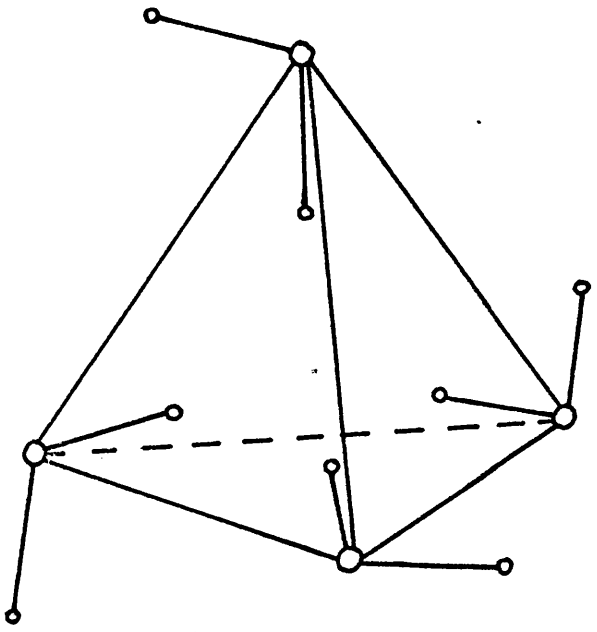

IX

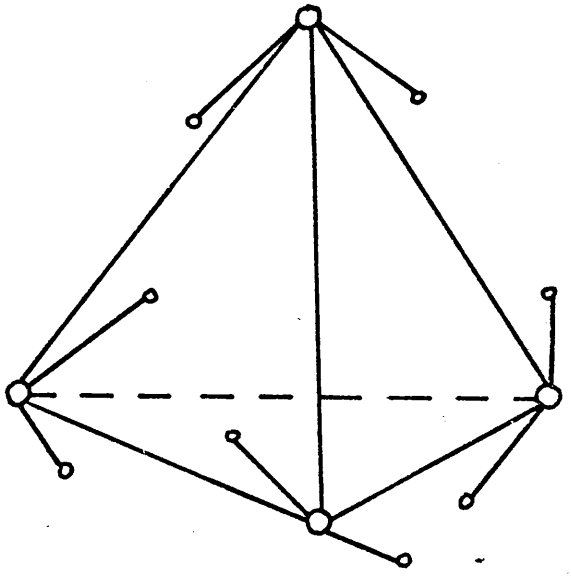

X

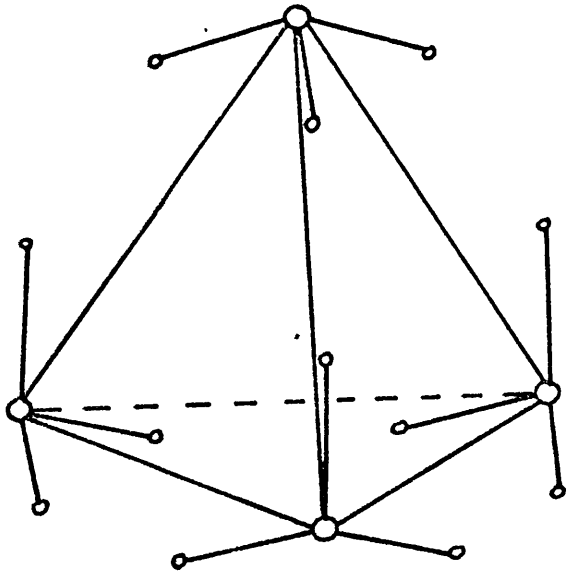

freezing point[17] suggests that the sites housing the electron are very similar. The low yield of trapped electrons in crystalline ice indicates a requirement for some pre-existing site at which the electron is established. Kawabata recently found that by doping ice crystals with fluorides, so enhancing the number of defect sites in some way, the yield of trapped electrons was dramatically increased.[18] EPR studies suggest that the site is water-walled[13] and coordinated by approximately four water molecules.[20]

Another model which may also satisfy these criteria is to be found in Figure 7, labelled IX. The eight protons of the surrounding water molecules point towards the centre of the tetrahedron. To construct a solvation shell of this form from the ice structure requires considerably more molecular reorientation around some vacant site.

The problem of alleviating the resulting proton-proton repulsions is achieved by rotation of each molecule until the sum of the intermolecular proton-proton distances is a maximum.

In the tetramer model X proposed for the ammoniated electron, the twelve protons lie between the nitrogen atom and the tetrahedron centre. It is difficult to relieve any proton-proton repulsions since a rotation of any molecule, increasing the distances between some nuclei, brings other repulsions into play.

This structure is necessarily an arbitrary choice. The number of molecules surrounding the localisation site of the ammoniated electron is known only to lie within a range 3 - 13.[15]

The INDO energies computed for the negatively charged tetramers at various distances from the centre to tetrahedron vertex, are collected in Table 7, and displayed in Figure 8. The reference state energy is highlighted on each diagram.

The hydrated electron structures VIII and IX exhibit an equilibrium geometry at D = 1.92Å and 1.85Å respectively. At the minimum energy, each structure is found to be stable with respect to the reference state energy -76.7424 a.u., model VIII by 2.22eV and model IX by 1.63eV.

This conclusion is at variance with the CNDO/2 studies of Weissman and Cohan.[7] At a distance D = 1.73Å, they report that structure VIII is energetically unfavourable by 0.40eV. The energy expended on forming this structure is 1.90eV while the electron affinity is placed at some 1.50eV below the electron affinity of the

Figure 8. The total energy variations for the tetramer structures with tetrahedron size. The appropriate reference states are highlighted by the broken lines.

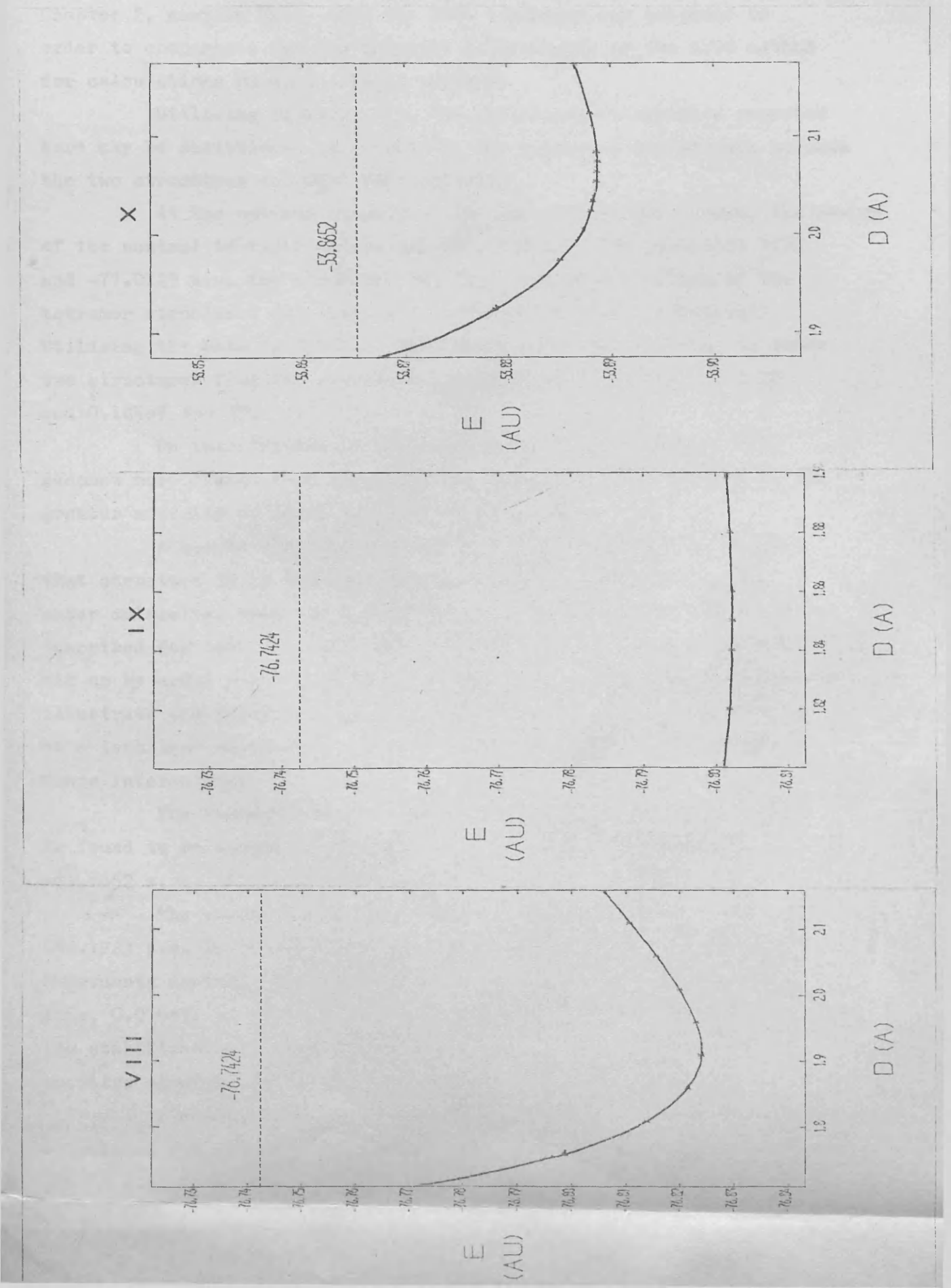

isolated water molecule.

It is the author's opinion that this conclusion may be a consequence of using the CNDO approximation. It may be recalled from Chapter 2, section D(i), that the INDO technique was proposed in order to compensate for the inherent deficiencies of the CNDO method for calculations on open - shell systems.

Utilising equation (2), the stabilisation energies reported here may be partitioned to illustrate the essential differences between the two structures and CNDO calculations.

At the optimum geometries for the charged structures, the energy of the neutral tetramer models are -77.0078 a.u. for structure VIII and -77.0129 a.u. for structure IX. The electron affinities of the tetramer structures are therefore 5.00eV and 5.73eV respectively. Utilising the data in Table 1, the energy gains on formation of these two structures from the separated components are 0.006eV for VIII and 0.145eV for IX.

On introduction of the surplus electron, structure VIII becomes more stable than structure IX, mainly as a consequence of the greater affinity of model VIII for an electron.

A simple electrostatic model might be expected to predict that structure IX is the most favourable arrangement of the four water molecules. When the dipole moments are aligned in the manner described for model IX, the potential well will be deeper than that set up by model VIII, leading to a lower energy. The INDO calculations illustrate the importance of investigating solvated electron models by a technique which will allow the detailed evaluation of short range interactions.

The tetramer model X proposed for the ammoniated electron is found to be stable by 0.63eV over the reference state energy -53.8652 a.u., at an equilibrium geometry of D = 2.07Å.

The energy of the uncharged structure at this geometry is -54.1223 a.u. By partitioning the stabilisation energy into the components defined in equation (2), it is found that a small energy gain, 0.076eV, is obtained on formation of the solvation shell. The low stabilisation energy arises as a result of the fairly large and positive electron affinity, 6.35eV, of the neutral structure.

Finally, it may be noted that the centre to vertex distances calculated for the tetramer structures are smaller than the centre to dipole distances obtained from the semicontinuum treatment described

in Chapter 3., Section E.

(ii) The Computed Excitation Energies for the Tetramer Models.

The calculated excitation energies for the three tetramer structures, VIII, IX and X, are assembled in Table 8.

At the optimum geometries, the excitation energies for the hydrated electron models VIII and IX are computed to be 2.08eV and 0.85eV respectively. The former value matches quite well with the observed absorption maximum of 1.72eV, while the latter is low.

Consider model VIII. If increases in temperature and pressure cause respectively expansion and contraction of the water cluster, the predicted shifts in the absorption spectrum are qualitatively in accord with experiment.

The contrasting behaviour of the transition energy for the two water clusters is shown in Figure 9. As the water cluster IX is compressed, the transition energy moves to longer wavelengths, while for structure VIII the shift is to the blue and levels off for distances less than $\sim 1.8\text{Å}$.

As a consequence of its higher energy, the charged structure IX might be expected to persist only at high temperatures. Therefore, at elevated temperatures, the blue shift in the absorption maximum with pressure might be expected to reverse its direction. The recent study of the absorption spectrum of the hydrated electron between -4° and 390°C did not detect any such effect.[21] It is interesting to note that at 390°C in supercritical water the absorption maximum of the optical spectrum lies at 0.93eV, although at this primitive level of the molecular approach, no direct assignment of structure can be made.

Structures intermediate between VIII and IX may develop as the temperature increases, moving the transition energies to longer wavelengths.

Utilising the data in Table 8 concerning the defect model VIII, an attempt to quantify the spectral shifts with temperature and pressure might be made if the size of the cluster is taken to depend on the temperature and pressure.

The first peak in the radial distribution curve for water manifests a temperature dependence of the form[11]

$$R(\text{Å}) = 2.83 + 0.0018t \qquad (3)$$

Figure 9. The variation of the calculated excitation energies, ΔE(eV), with the distance D(Å) from the tetrahedron centre to the vertex for structures VIII and IX. The arrowed positions show the excitation energies at the optimum geometries.

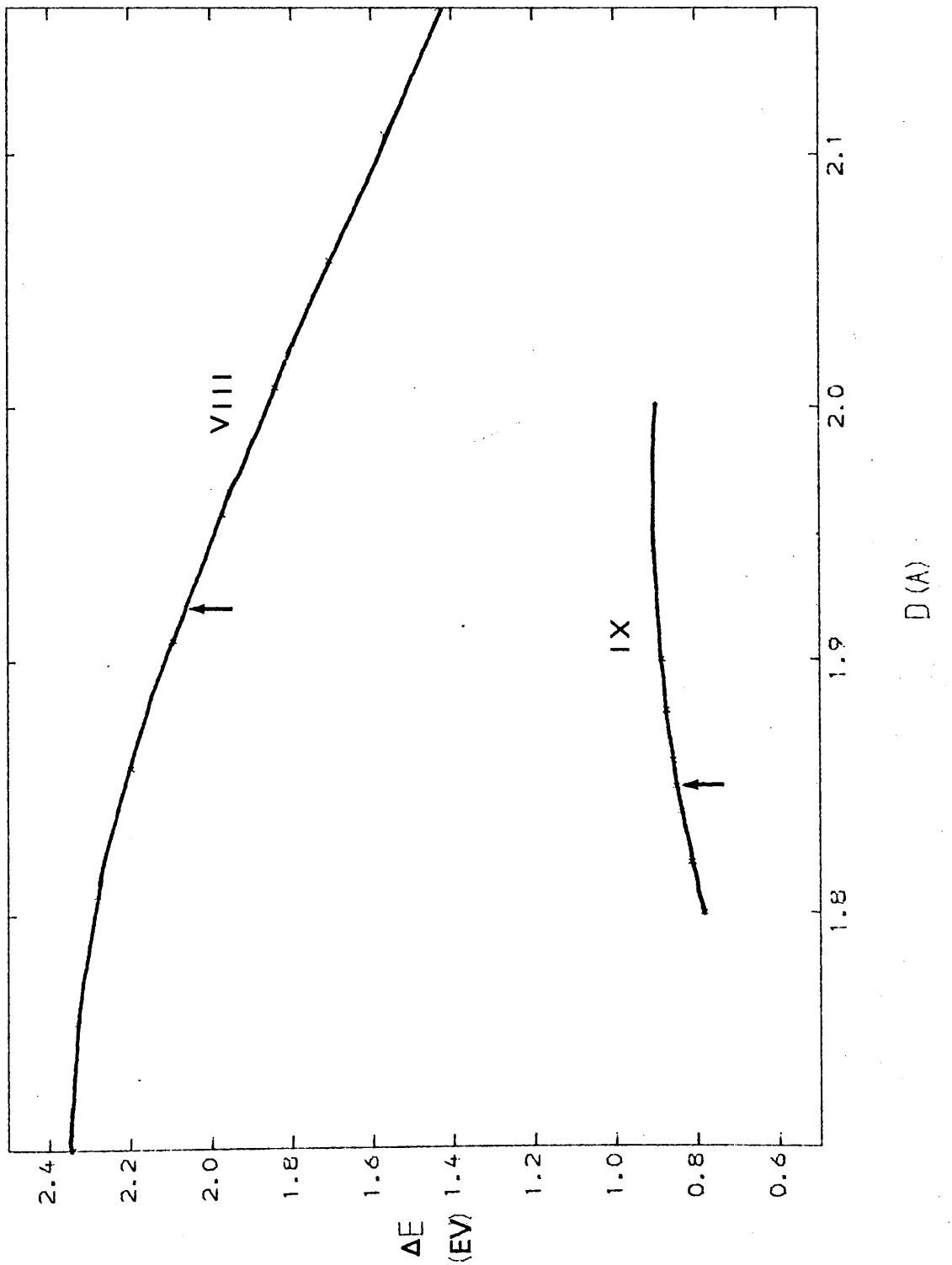

where t is the temperature in ^{o}C. The separation between nearest neighbour oxygen atoms increases with temperature at a rate $0.0018\text{Å}/^{o}K$. The water cluster VIII may be assumed to have a thermal expansion coefficient of this order by recognition that the localised electron might simulate the behaviour of the absent oxygen atom in the hydrogen - bonded water structure.

Close to the lowest energy geometry, D = 1.92Å, the excitation energy varies with cluster size as $dE_{max}/dD = -2.23eV/\text{Å}$. Combined with the thermal expansion coefficient of the cluster, the computed temperature dependence of the peak position is

$$d E_{max}/ dT = (d E_{max} / dD . dD/dT) = -0.0040eV/^{o}K.$$

A similar calculation for the planar dimer model I yields a value $- 0.0032$ eV / ^{o}K. Over the range $0^{o} - 90^{o}C$, Gottschall and Hart[5] found that the absorption maximum for the hydrated electron has a temperature coefficient of $-0.0029eV/^{o}K$. The theoretical shift is in fair agreement with the experimental observation.

The temperature coefficient in ice[17] is $-0.0012eV/^{o}K$, lower than that in water. The average oxygen to oxygen distance in ice is less temperature dependent than in water. From the x-ray data of La Placa and Post,[22] between $-10^{o}C$ and $0^{o}C$ the average thermal expansion coefficient of ice is $\sim 0.00016\text{Å}/^{o}K$. The calculated temperature coefficient of the absorption maximum in ice may then be placed at $dE_{max}/dT = -0.00035eV/^{o}K$, a factor of three smaller than the observed value.

At $24^{o}C$, if the applied pressure is raised to 1000 atmospheres, the average oxygen - oxygen distance in water decreases from 2.873Å to 2.825Å.[23] Taking the size of the tetramer to vary at a rate $(2.825 - 2.873)\text{Å}/kbar$, the pressure coefficient of the absorption maximum is calculated to be 0.085eV/kbar. The trend in the excitation energy, displayed in Figure 9 for structure VIII, shows that this pressure coefficient should fall off as the cluster is compressed.

Experimentally, the pressure coefficient is observed to be 0.053 - 0.06eV/kbar for pressures up to approximately 5kbar. At pressures in excess of 5kbar, further increases have little effect on the spectrum.[24]

These calculations assume that the spectral shifts with

pressure and temperature are determined mainly by variations in the dimensions of the cluster. Effects which may arise from reorientation of the coordination shell have not been considered quantitatively. Despite the approximations involved, the qualitative and quantitative conclusions which may be drawn match quite well the observed spectral phenomena for the hydrated electron. We now consider the ammoniated electron structure X.

At the equilibrium geometry D = 2.07Å, the ammonia tetramer model exhibits an excitation energy of 0.72eV, slightly lower than the observed value 0.80eV at 240°K.[10] The temperature coefficient of the absorption maximum is $-1.5 \pm 0.2 \times 10^{-3}$ eV/°K.

As the cluster size decreases, the calculated excitation energies shift to the blue, qualitatively in accord with the effects of pressure on the spectrum.[25]

From x-ray diffraction experiments,[12] each molecule in ammonia at 199°K is surrounded by approximately seven molecules at a distance 3.56Å, with four more at 4.1Å. Raising the temperature to 277°K increases the former distance to ~ 3.74Å. The latter value should be regarded as an estimate, since it was obtained from the radial distribution curves published by Kruh and Petz.[12]

Setting the thermal expansion coefficient of the tetramer to (3.74 - 3.56)/(277 - 199) = 0.0026Å/°K, the temperature coefficient of the absorption maximum is calculated to be -0.002eV/°K, in good agreement with experiment. A similar calculation for dimer structure II affords an estimate -0.0065eV/°K.

(iii) The Bandwidth of the Hydrated and Ammoniated Electron Optical Spectrum.

For the single configurational coordinate D, the predicted band shape is determined by the thermal population of a configuration and the transition energy at that configuration. Measured from the minimum energy E_{min}, the half band - width at high temperatures T, is determined from the points D_1 and D_2 for which

$$E(D_1) - E_{min} = E(D_2) - E_{min} \approx kT \qquad D_2 > D_1$$

where k is the Boltzmann constant. The half bandwidth is then given

Figure 10. The breakdown of the optical absorption spectrum of the ammoniated electron at 258°K (from ref. 33) following the method of Hamill (ref. 29). The full line shows the observed spectrum.

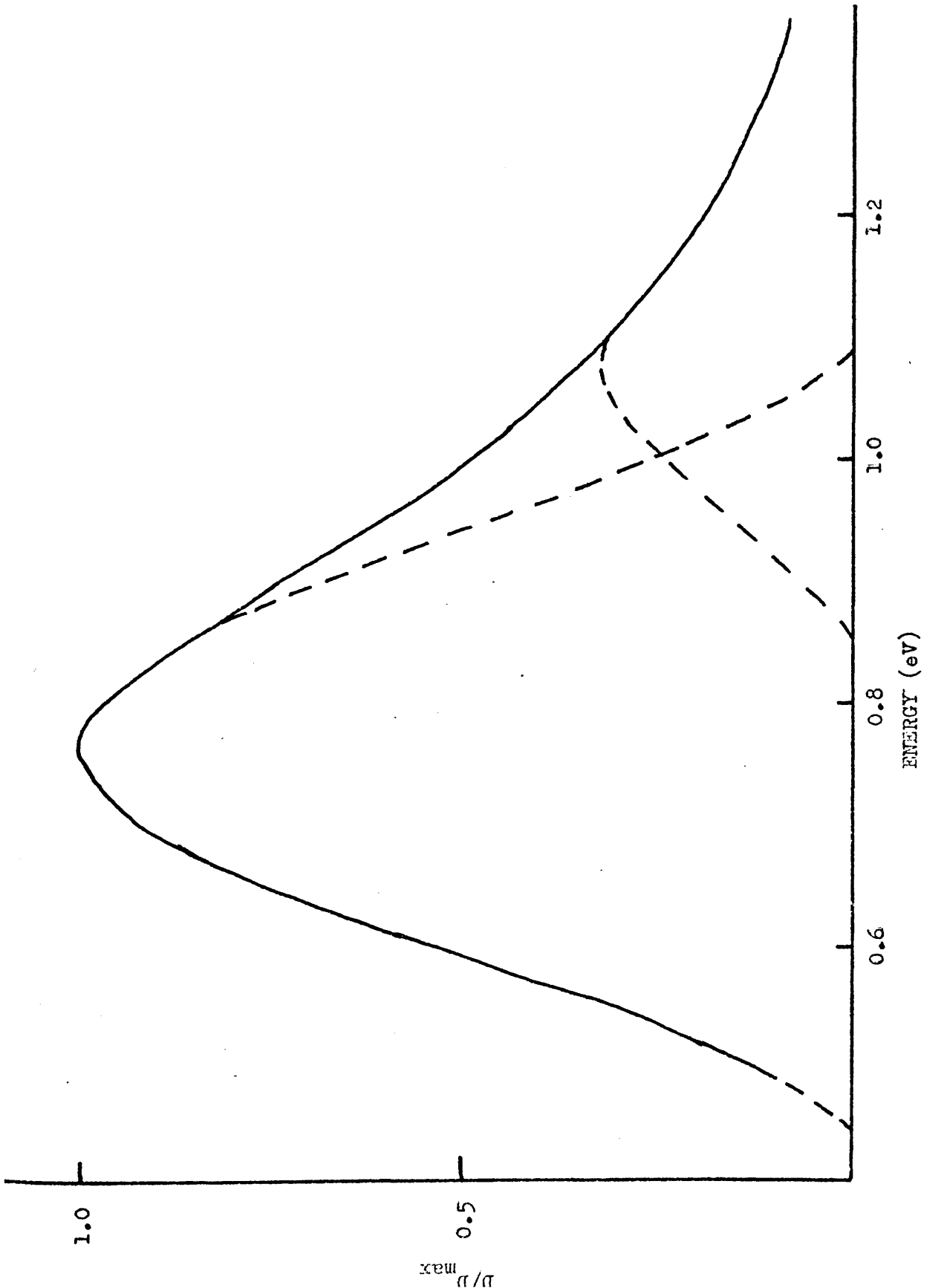

by

$$W_{\frac{1}{2}} = |E_{ex}(D_1) - E_{ex}(D_2)|,$$

where $E_{ex}(D_1)$ is the computed transition energy at D_1.

The half bandwidths calculated in this way are 0.1eV for structure VIII at 300°K and 0.08eV for structure X at 240°K. The observed half bandwidths of the solvated electron spectra are somewhat larger, 0.56eV in ice (77°K),[18] 0.92eV in water (300°K)[26] and 0.46eV in ammonia (240°K).[10]

This discrepancy concerning the width is also a feature of the semicontinuum treatment.[27]

A rationalisation of the observed band shape is achieved by proposing that a variety of different trapping sites around the optimum exist in the liquid[28] or that the observed spectrum is the envelope of several absorption bands[27] arising from several excitations. The true situation probably combines both features.

In support of the second alternative, Hamill[29] showed that the shape of the absorption spectrum of the trapped electron in 3-methylpentane is consistent with the overlapping of two excitation bands.

Following Hamill, the absorption spectrum of the ammoniated electron at -15°C, shown in Figure 10, may be considered to be the envelope of two absorption bands, one at 0.77eV and another at 1.08eV, with the indication of further bands or a continuous absorption at higher energies. This breakdown is achieved by reflection of the lower energy edge of the band and subtraction of the intensity from the total intensity.

If the higher energy absorption at 1.08eV arises from a 1s to 3p transition, the polarised cavity model may be utilised to estimate the energy for such a process. With $D_{op} = 1.756$ and $D_{st} = 22$, equation (18) places the 3p level at an energy -0.783eV. For a cavity radius of 3.2Å, the ground state energy is -2.073eV. The 1s to 3p transition should therefore lie at 1.29eV, in good agreement with the high energy peak in Figure 10.

The half bandwidth of the first excitation band is 0.36eV, a fair reduction over the total bandwidth. This value is still larger by a factor of ~4 than the tetramer model calculation suggests.

The observation that the large bandwidth in water, 0.92eV, falls to 0.56eV in ice perhaps suggests that there is a wider range of similar traps in water. To account fully for the observed bandwidth would therefore appear to be futile unless both the distribution of traps and higher energy absorption processes are taken into account.

(iv) Dilation Phenomena.

The volume increments associated with the surplus electron have recently been measured to be 84 ± 15 ml/mole (240°K) in ammonia and 20 ml/mole,[25] 1 - 6 ml/mole[30] in water. The impact of such phenomena on the theoretical models for the solvated electron is reflected by the inclusion of a parameter which describes the effective radius of a void volume. The molecular approach introduces a new factor to be considered.

Consider structure VIII for the hydrated electron. In the absence of the surplus electron, the lowest energy geometry lies at D = 2.11Å. Introduction of the electron contracts this distance to 1.92Å, as already mentioned in Section C (i). This feature suggests that volume increments may be a manifestation of some other phenomenon than cavity formation, for example, the whole lattice about the localisation site may be expanded. Alternatively, the region surrounding the site may be diluted compared to the normal liquid.[30]

Developing the former concept, four molecules in water may be situated at the corners of a tetrahedron fixed in a cube of volume 119.56Å.^{3} In the prescence of the electron, this cell expands by a distance (1.92 - 0.958)Å in each direction, aquiring a volume 320.01Å.^{3} The volume expansion is therefore 30.19 ml/mole. Treating the ammonia tetramer structure in this way predicts a volume expansion of 81 ml/mole, for an ammonia density of 0.6814 g/ml at 240°K.

No cavities are formed in the liquid. An excluded volume is created within which the molecules coordinating the centre may not enter, thus expanding the volume associated with each cluster.

In a more conventional way, the molecules could be ascribed a radius r, beyond which lies the second solvation shell. Taking r = 1.5Å for ammonia and water, as suggested by Copeland et al,[27] the spherical region associated with the tetramers may be ascribed a volume 167.56Å^3 for structure VIII and 190.59Å^3 for structure X.

The volume increments associated with the surplus electron in water and ammonia are 28.9 ml/mole and 20.9 ml/mole respectively. The observed magnitudes are in the reverse for these solvents.

The relationship between these two viewpoints may be seen if the lattice expansion is treated as crudely equivalent to an expansion of the molecular radii in the prescence of the electron. The consideration of models which include a second solvation shell would be an interesting test of the lattice expansion concept.

(v) The Ammonia - Water Mixed Solvent System.

The polaron theory qualitatively accomodates the observation than an increase in solvent polarity leads to a peak absorption for the solvated electron at shorter wavelengths. By sampling a large portion of the medium the electron is expected to exhibit a compromise spectrum lying between the spectra of the pure components. The studies of Arai and Sauer[32] and of Dye, DeBacker and Dorfman[33] were instigated to investigate this behaviour in alcohol-water and amine-water solutions respectively. In both cases it is concluded that the solvated electron interacts with a large number of molecules.

Yet there is some evidence that the formation of aggregates of polar molecules is important to stabilise the electron in mixtures of polar-non-polar mixtures.[34] Two absorption peaks, characteristic of the pure liquids, are observed.[35]

It is of interest and desireable, as a test of the molecular approach, to investigate the manner in which the tetramer models portray the behaviour of the surplus electron spectra in ammonia-water solutions. Tetramer aggregates which might be important at different mole fractions of water are illustrated in Figure 11. Each structure is obtained by successive replacement of one water molecule in structure VIII by an ammonia molecule oriented as in structure X. The computed ground state and transition energies are collected in Table 9.

The excitation energies computed at the lowest energy geometry for each structure are superimposed on the experimental data observed by Dye, DeBacker and Dorfman in Figure 12. The computed energies vary non-linearly between the limiting excitation energies for the pure tetramer models. Although the match of these two curves is not quantitative, the overall trend in the excitation energy of the surplus electron is well reproduced by the calculations.

Figure 11. The tetramer structures utilised to represent the molecular clusters occuring in ammonia - water mixtures at various mole fractions, x, of water.

x = 0.75

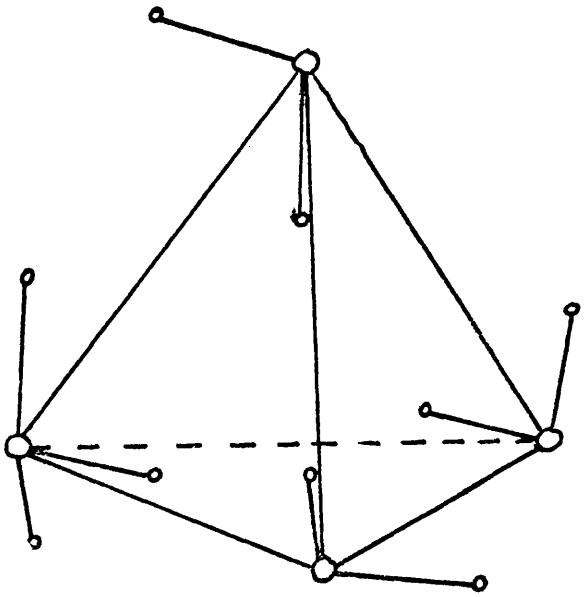

x = 0.5

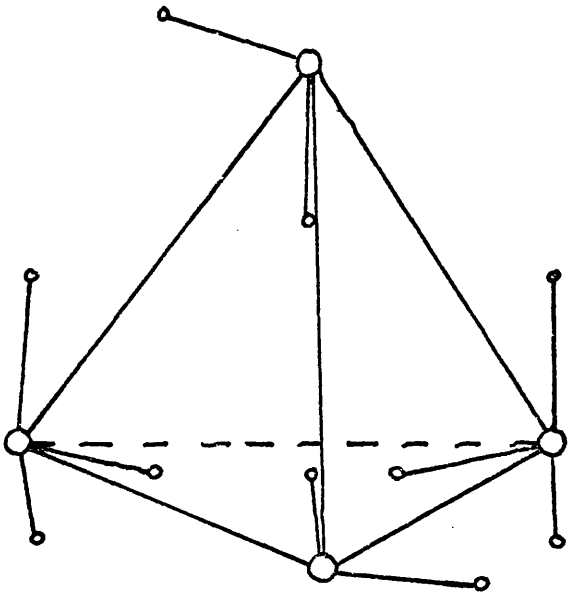

x = 0.25

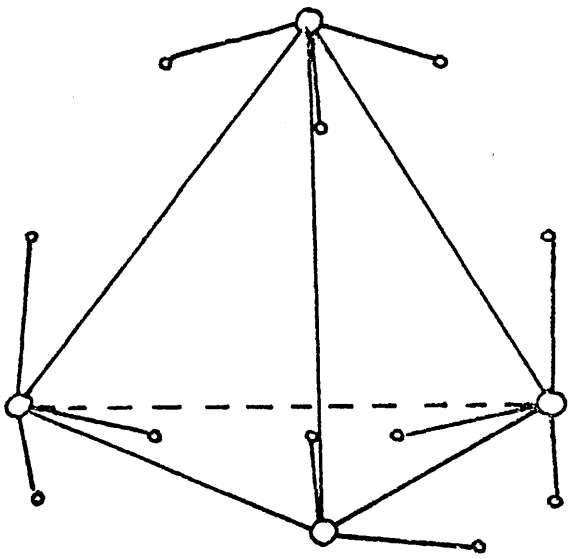

Figure 12. The computed and observed excitation energies of the surplus electron in ammonia - water mixtures. The full line shows the experimental data; the crosses mark the calculated transition energies at 5 mole fractions of water.

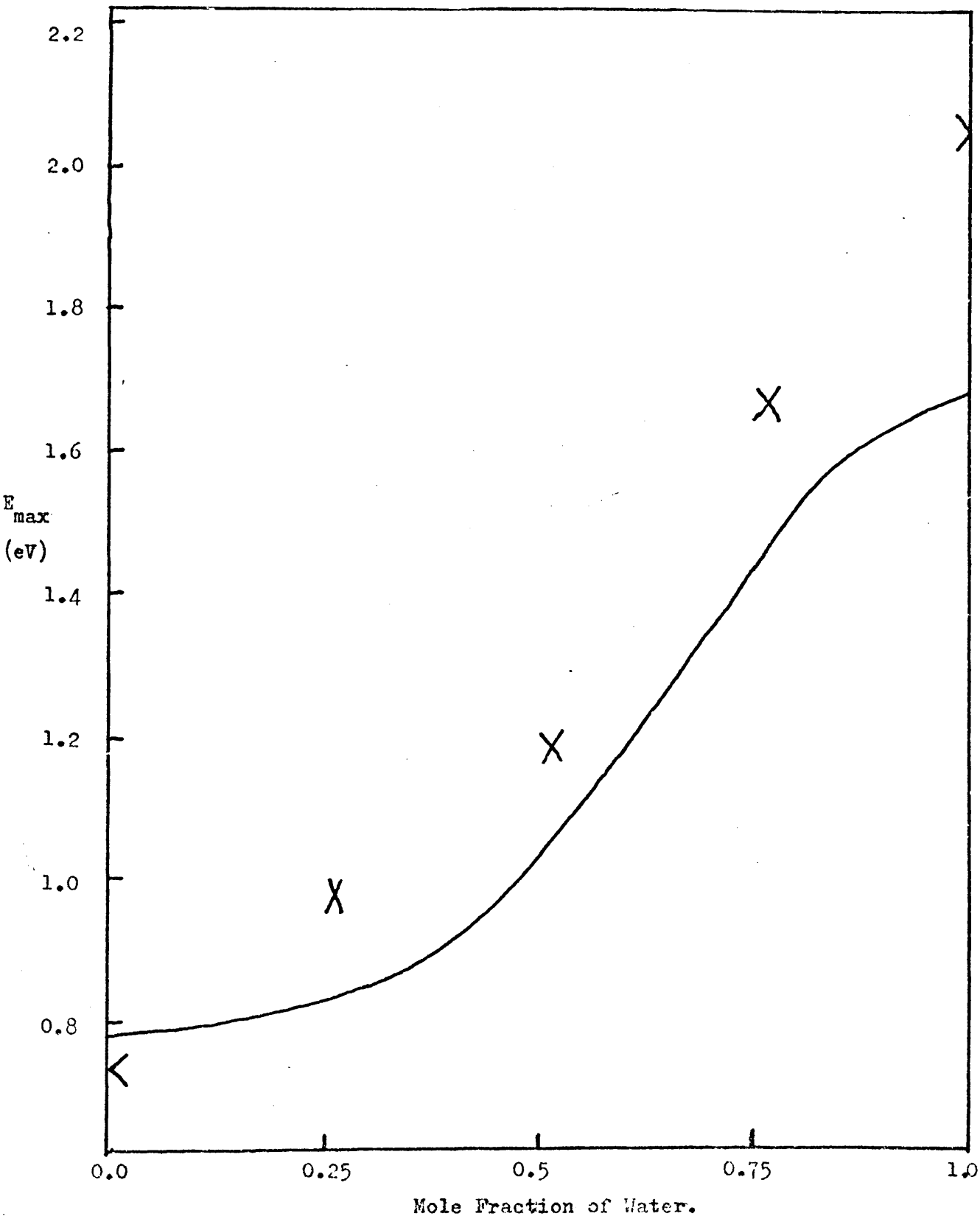

Examination of the total energy for each tetramer shows that there is a progressive decrease in the stabilisation energy over the reference state as each water molecule is replaced. For example, on moving from $(NH_3, 3H_2O).\ e^-$ to $(2NH_3, 2H_2O).e^-$ the decrease in stabilisation energy is 0.5leV. The energy of the mixed structures is to be compared with two reference states, depending on whether the surplus electron is formally associated with an ammonia or a water molecule.

As ammonia molecules are added, the cluster in general expands, excepting that a small contraction is observed at a mole fraction of water 0.75.

(vi) The Charge Distributions.

The calculated excess electron density at each atom for for the tetramer models VIII to X is portrayed in Figure 13. As was observed with the dimer structures I and II, the electron is delocalised over the cluster. Protons lying closest to the centre of the tetrahedron acquire more charge than the more distant protons. It is also in evidence that the hetero-atoms retain most of the electron density, the overall average value being $0.16e^-$.

One of the important features of the molecular approach is that spin densities at nuclei comprising the cluster are readily obtained. Earlier treatments relied on orthogonalising the wave function obtained from a cavity model calculation with the peripheral solvent orbitals.[36] The INDO molecular orbital treatment includes spin polarisation in a natural way.

By comparison with some experimental data from magnetic resonance experiments, the grain of the molecular orbitals might be examined.

(vii) The Electron Spin Resonance Spectrum of the Solvated Electron.

(a) Introduction.

The electron spin resonance spectrum of the solvated electron in polar media is typified by a single resonance. Linewidths vary from the fine, 0.02 gauss in liquid ammonia at 293°K,[37] to the broad, greater than 50 gauss for caesium in methylamine.[38]

The origin of this narrow absorption has been interpreted in two ways. Kaplan and Kittel[2] proposed that hyperfine interactions of

Figure 13. The calculated charge densities of the excess electron at each atom in the tetramer structures VIII, IX and X.

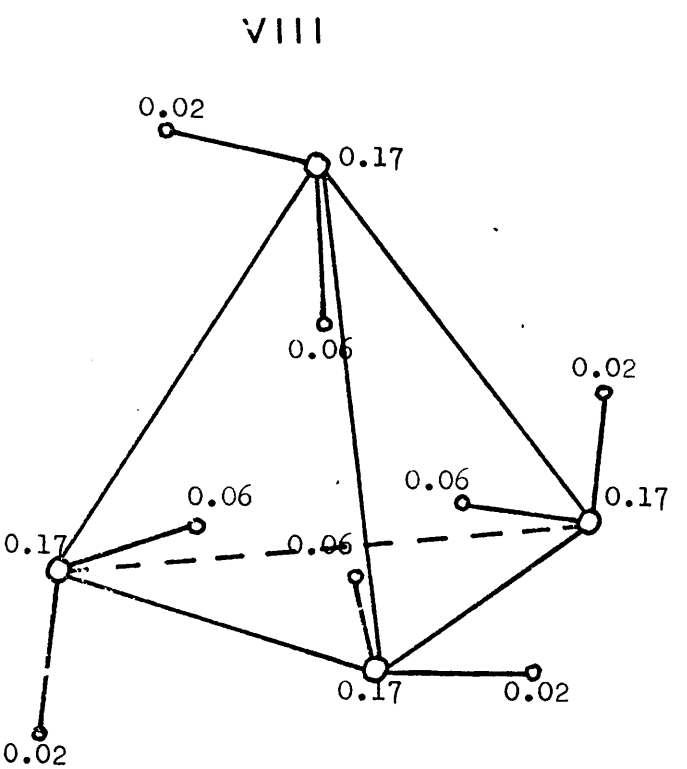

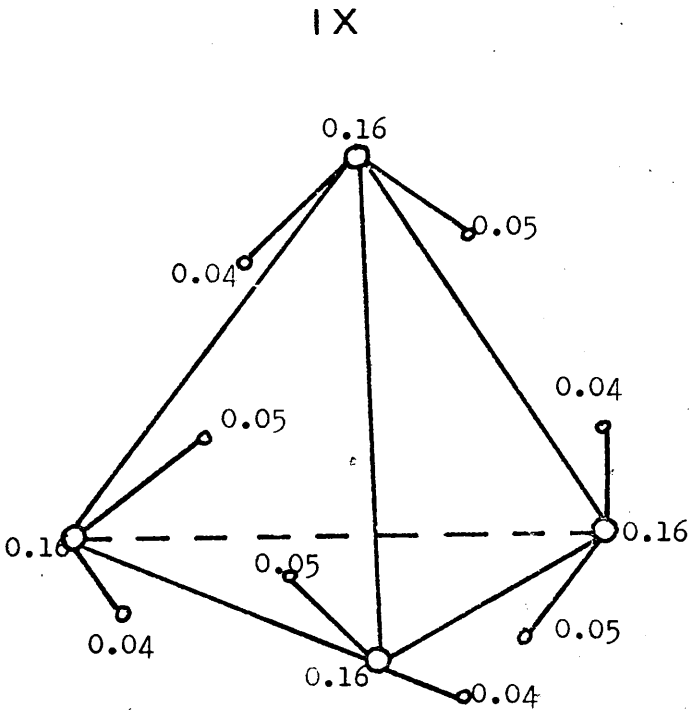

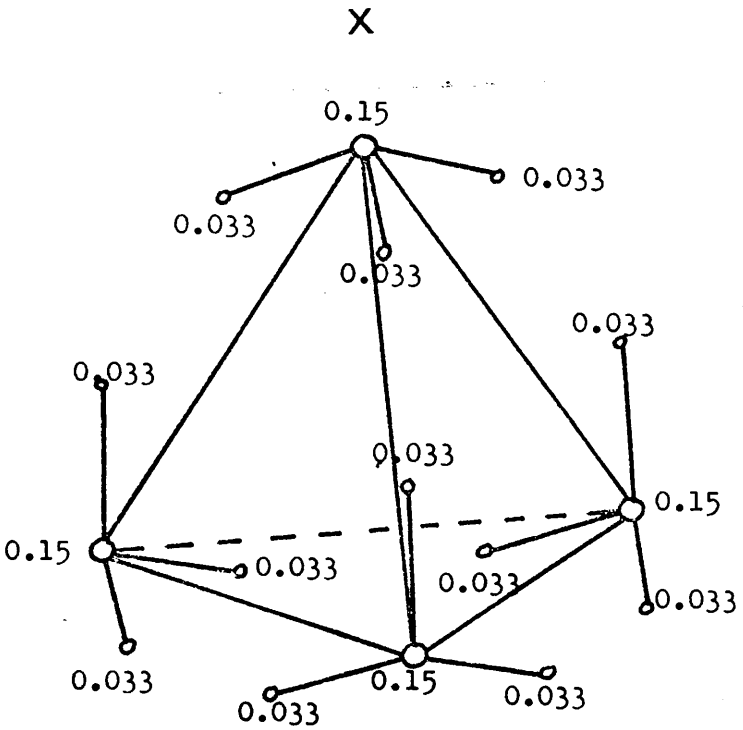

the surplus electron with the protons in ammonia were rapidly modulated by the Brownian motion of the medium molecules. Subsequent NMR measurements were at variance with this proposal,[39] while isotopic substitution of ammonia revealed the predominant origin of the residual broadening to be due to hyperfine interaction with nitrogen nuclei.[40,41] The relaxation mechansim has also been considered as a manifestation of tunnelling effects which modulate the hyperfine interactions.[15,41,42].

The alternative approach views the solvated electron as a polaron. Deigen and Pekar[43] showed that to a first approximation, hyperfine interactions do not alter the energy of the polaron. Consequently no broadening of the ESR spectrum will be observed. The extreme sharpness of the linewidth in metal-ammonai solutions is held as evidence for the existance of the polaron in this medium. The observation of such hyperfine interactions invalidates this conclusion.

The importance of hyperfine interactions with protons is demonstrated by the spectra of alkaline aqueous glasses[44] and glassy alcohols.[45] In the deuterated medium the linewidths of the spectra are more than halved from 15 to 7 gauss.

The ESR spectrum has not yet been observed in pure ice, although in water at 5°C the linewidth is reported to be < 0.5 gauss.[46] Recalling the correspondance between the structure of the solvated electron in ice, alkaline glass and water (cf. Section C (i)) it would appear that the narrow linewidth in water is a result of modulation of the hyperfine interactions with protons.

(b) Theoretical Considerations.

When the ESR spectrum is assembled from the envelope of absorptions arising from hyperfine interactions with various different nuclei, the calculation of the linewidth for a rigid lattice is relatively simple. The root mean square linewidth may be assessed by the relation[47]

$$W^2 = 64\,\pi^2 \,/\, 27 \sum_i \mu_i^2 \frac{I_i + 1}{I_i} \rho_i^2 \text{ gauss} \qquad (4)$$

where μ_i is the magnetic moment of nucleus i with spin I_i. ρ_i is the unpaired spin density at nucleus i. This expression has been utilised by Kevan[20] to illustrate that the linewidth of the ESR spectrum in γ-irradiated alkaline glasses arises from the interaction of the

electron with approximately eight protons.

Equation (4) is applicable to a rigid lattice. When the hyperfine interaction fluctuates at a rate τ_c^{-1}, the linewidth is modified and may be calculated from the relation[48]

$$\delta H = \gamma W^2 \tau_c \quad \text{gauss.} \qquad (5)$$

where γ is the electron gyromagnetic ratio.

The value adopted for the correlation time τ_c is critical. To make an estimate, the relaxation mechanism must be known.

Nuclear magnetic resonance studies by Catterall, Stodulski and Symons concluded that the modulation of the contact interactions proceeds more rapidly than viscosity controlled molecular process.[40] It is therefore surprising that the linewidth variations of dilute sodium-ammonia solutions with temperature are accommodated utilising a correlation time proportional to η/T where η is the viscosity of the medium.[15,42]

For these reasons, upper limits to the correlation time are estimated. The correlation time for restricted rotation of ammonia molecules in the liquid at 293°K is estimated from the Debye relation to be 4.8 picosec.[50] The Debye formula is found to hold when the tumbling species is approximately spherical and ~3 times larger than the solvent molecules.[51] When some account of the molecular nature of the medium is taken, the predicted correlation times are reduced by a factor of 5 - 6 times,[52] for ammonia to ~0.96 psec.

Utilising an equation between the correlation time for dielectric relaxation and viscosity reported by Grant,[53] τ_c for water at 5°C is taken to be 13.6 psec.

(c) The Linewidth Calculations.

The INDO calculations utilise a basis set consisting of Slater functions. Consequently, the node in the 2s functions for first row atoms is collapsed to a point node at the nucleus and spin densities at the nucleus are not immediately available within the INDO method. Recognising this defect, Pople, Beveridge and Dobosh[54] showed that the spin densities at nitrogen and hydrogen nuclei may be estimated from the semi-empirical relations

$$\rho_N = 22.2168\ R_{2s\ 2s} \times 10^{24}\ cm^{-3}$$

$$\rho_H = 2.2811\ R_{1s\ 1s} \times 10^{24}\ cm^{-3}$$

where the spin density matrix elements R_{pq} are given by

$$R_{pq} = P^{\alpha}_{pq} - P^{\beta}_{pq}.$$

Table 10 displays the spin densities so computed at various nuclei for the tetramer models VIII to X. The total spin densities are compared with the observed values in alkaline ices[20,55] and metal-ammonia solutions.[15]

In general the spin density at the protons is somewhat overestimated by a factor of about four in the hydrated electron models. The small negative spin density observed at the ammonia protons is not at all well reproduced, the calculated value being about 0.9. The calculated density at nitrogen nuclei is of the correct magnitude.

Negative spin densities at protons are also observed in metal-amine solutions.[56] This feature is not an uncommon phenomenon for organic radicals. Usually some spin polarisation mechanism is indicated.

Using equations (4) and (5) and the data in Table 10, the ESR linewidths were calculated for a range of correlation times. Computed and experimental values are collated in Table 11.

For the hydrated electron, the agreement with the currently available experimental data[46] is fair. On deuteration, the linewidth is predicted to decrease markedly.

For the ammoniated electron, the calculated linewidth is of the correct order of magnitude, the dominant interaction being with the nitrogen nuclei. The linewidth is predicted to decrease in deuteroammonia. Recalling that the spin density in metal-ammonia solutions is found to be negative, with a comparable correlation time in deuteroammonia the linewidth should increase over that observed in ammonia. Taking the correlation time to be proportional to η/T, τ_c in ND_3 is increased by a factor of ~ 1.2 over that in NH_3.[41] The calculated difference in linewidths between the two solvents then becomes smaller.

That the predominant hyperfine interactions in ammonia solutions are with the nitrogen nuclei is well accounted for within

the INDO calculations. The discrepancy concerning the sign of the density at protons may be a fault of the simple tetramer model proposed for the ammoniated electron. The introduction of larger coordination shells or further coordination shells may indeed be required to describe the electron - proton interactions more fully.

In addition, the molecular orbitals of the system are constructed from a minimal basis set of atomic orbitals centred on each atom. It may be necessary to introduce more flexibility into this set by including more atomic orbitals or functions which stem from the centre of the tetramer. Spin density may then be better represented.

Parametrisation of these orbitals within the INDO approximation is a very difficult process. An attempt to introduce 2p functions on the hydrogen atoms met with complete failure. An ab initio UHF calculation on the ammonia tetramer may be the only way round this problem.

(viii) The Tetramer Model Calculations and the Semicontinuum Treatment.

To summarise the calculations on the tetramer models for the solvated electron, Table 12 collates the calculated and observed properties of the hydrated electron (structure VIII) and the ammoniated electron (structure X). The data in this table may be compared with that in Table 1 of Chapter 3.

Both the molecular approach and the semicontinuum treatment provide a reasonable match with experimental data when the same property is considered, in particular spectral observations. However, within the molecular approach, it is difficult to predict such a property as the heat of solvation. This calculation would involve some consideration of the liquid surrounding the molecular cluster. The molecular orbital calculations are necessarily performed for the isolated cluster, although a correspondance with the liquid state is claimed. This problem must await further developments.

It is unfortunate that some recourse must be made to experimental observations on the pure liquids in order to quantify the spectral shifts with temperature and pressure. This feature of the molecular approach arises since the configuration diagram is not temperature or pressure dependent, as in the semicontinuum treatment. The molecules comprising each cluster are held rigidly at the vertices

of the tetrahedron. Temperature and pressure effects are then assumed to expand or contract the tetramer. Yet even so, some experimental observations have been shown to be well accommodated in this simple fashion.

A particularly important facet of the molecular orbital treatment is that spin polarisation effects may be immediately investigated. Although the INDO spin densities at the cluster protons are somewhat higher than the observed values, it is recognised that a more refined computational technique or a more elaborate model structure may be required to produce closer agreement with experiment. The semicontinuum treatment cannot account for this feature.

Some discrepancies still remain within the molecular approach, particularly those concerning the bandwidth. The analysis of the bandshape of the ammoniated electron, section (iv), demonstrates that this deficiency may not be as severe as first supposed. There would appear to be a range of different clusters around the optimum geometry which the molecular approach does not accommodate. For each tetramer model a unique cluster size is predicted.

The successes of the two approaches to the treatment of the solvated electron recommend that perhaps both treatments should be utilised in a complementary fashion. The semicontinuum treatment may be useful to gauge the gross properties of the solvated electron, while the molecular approach utilised to refine the model. The theory may also be further advanced by some fusion of the two approaches as was performed by Jortner in the formulation of the polarised cavity model.

TABLE 2

The calculated energies E(a.u.), for the planar structures I and II for various intermolecular separations D(Å).

I		II	
D	E	D	E
1.0	-38.2683	1.0	-26.8179
1.1	-38.2764	1.1	-26.8275
1.2	-38.2787	1.2	-26.8321
1.3	-38.2781	1.3	-26.8337
1.4	-38.2757	1.4	-26.8334
1.5	-38.2723	1.5	-26.8321
1.6	-38.2687	1.6	-26.8304
1.7	-38.2649	1.8	-26.8265
		2.0	-26.8230

TABLE 3

The calculated energies E(a.u.), for the ice-like fragment III for various intermolecular separations D(Å)and angles α°.

D/α	0	15	30	45	60	75	90
1.1	-38.2942	-38.2938	-38.2925	-38.2902	-38.2862	-38.2796	
1.15	-38.3069	-38.3073	-38.3064	-38.3042	-38.3010	-38.2951	
1.2	-38.3158	-38.3154	-38.3147	-38.3130	-38.3101	-38.3051	-38.2974
1.25	-38.3198	-38.3195	-38.3189	-38.3175	-38.3151	-38.3107	
1.3	-38.3207	-38.3205	-38.3200	-38.3189	-38.3168	-38.3131	-38.3074
1.35	-38.3195	-38.3193	-38.3189	-38.3179	-38.3162	-38.3132	-38.3085
1.4	-38.3170	-38.3166	-38.3162	-38.3154	-38.3140	-38.3115	-38.3074
1.5		-38.3087	-38.3084	-38.3075	-38.3069	-38.3085	-38.3022

TABLE 4

The calculated excitation energies E_{ex}(eV) for various intermolecular separations D(Å) of the dimer structures I and II.

I		II	
D	E_{ex}	D	E_{ex}
1.0	2.32	1.0	1.53
1.1	2.16	1.1	1.38
1.2	1.98	1.2	1.23
1.3	1.80	1.3	1.10
1.4	1.63	1.4	0.98
1.5	1.46	1.5	0.87
1.6	1.30	1.6	0.77
1.7	1.15	1.8	0.59
		2.0	0.45

TABLE 5

The calculated excitation energies in eV for the ice-like structure III at various intermolecular separations D(Å) and angles α°.

D/α	0	15	30	45	60	75	90
1.1	7.20	7.25	7.36	7.50	7.60	7.61	
1.15		6.92	7.00	7.14	7.22	7.23	
1.2	6.50	6.57	6.66	6.75	6.85	6.84	6.72
1.25	6.18	6.21	6.29	6.40	6.47	6.46	
1.3	5.82	5.85	5.97	6.03	6.10	6.09	5.99
1.35	5.47	5.50	5.58	5.67	5.73	5.72	5.63
1.4	5.13	5.16	5.23	5.32	5.38	5.37	5.29
1.5		4.52	4.59	4.66	4.72	4.75	4.65

TABLE 6

The calculated energies E(a.u.) for the dimer structures IV, V, VI and VIII at various separations D(Å). E_{ref} is the reference state energy.

IV

D	E
2.2	-38.1496
2.4	-38.1989
2.6	-38.2125
2.7	-38.2133
2.8	-38.2124
2.9	-38.2098
3.0	-38.2075
E_{ref}	-38.2386

V

D	E
2.0	-38.1880
2.2	-38.2245
2.4	-38.2372
2.5	-38.2385
2.6	-38.2388
2.7	-38.2382
2.8	-38.2371
	-38.2386

VI

D	E
2.1	-26.8030
2.2	-26.8034
2.3	-26.8035
2.4	-26.8033
2.5	-26.8030
E_{ref}	-26.8055

VII

D	E
2.0	-26.8007
2.1	-26.8018
2.2	-26.8024
2.3	-26.8025_9
2.4	-26.8025_6
	-26.8055

TABLE 7

The calculated total energies E(a.u.) for the tetramer structures VIII, IX and X. D(Å) is the distance from the centre of the tetrahedron to the vertex.

VIII		IX		X	
D	E	D	E	D	E
1.758	-76.7989	1.80	-76.8013	1.874	-53.8674
1.808	-76.8141	1.82	-76.8020	1.924	-53.8789
1.858	-76.8217	1.84	-76.8024	1.974	-53.8852
1.908	-76.8241	1.85	-76.8025	2.024	-53.8882
1.958	-76.8232	1.86	-76.8024	2.034	-53.8884
2.008	-76.8202	1.88	-76.8021	2.054	-53.8887
2.058	-76.8159	1.90	-76.8017	2.064	-53.8887_5
2.108	-76.8109	1.94	-76.8002	2.074	-53.8888
2.158	-76.8057	2.00	-76.7970	2.084	-53.8887_2
				2.124	-53.8881
				2.174	-53.8866

TABLE 8

The computed excitation energies E_{ex}(eV) for the tetramer structures VIII, IX and X. D(Å) is the distance from the tetrahedron centre to the vertex.

VIII		IX		X	
D	E_{ex}	D	E_{ex}	D	E_{ex}
1.758	2.33	1.80	0.78	1.874	0.87
1.808	2.28	1.82	0.81	1.924	0.84
1.858	2.20	1.84	0.84	1.974	0.80
1.908	2.09	1.85	0.85	2.024	0.76
1.958	1.97	1.86	0.86	2.034	0.75
2.008	1.84	1.88	0.87	2.054	0.74
2.058	1.71	1.90	0.89	2.064	0.73
2.108	1.57	1.94	0.90	2.074	0.72
2.158	1.53	2.00	0.90	2.084	0.71
				2.124	0.68
				2.174	0.64

TABLE 9

The computed total energies, E(a.u.), and excitation energies, E_{ex}(eV), for the ammonia - water tetramers. D(Å) is the distance from the tetrahedron centre to the vertices; n is the number of ammonia molecules substituted in structure VIII; E_1 and E_2 are the reference state energies when the electron is associated with a water and an ammonia molecule respectively.

n=1			n=2		
D	E	E_{ex}	D	E	E_{ex}
1.874	-71.0885_8	1.72	1.874	-65.3467	1.23
1.879	-71.0886_1	1.71	1.924	-65.3479	1.19
1.884	-71.0886_2	1.70	1.934	-65.3480	1.18
1.889	-71.0886	1.69	1.944	-65.3479	1.17
1.894	-71.0885_7	1.68	1.954	-65.3478	1.16
1.924	-71.0879	1.63	1.974	-65.3475	1.14
1.974	-71.0856	1.55			
E_1	-71.0204			-65.2984	
E_2	-71.0312			-65.3092	

n=3		
D	E	E_{ex}
1.874	-59.6000	1.02
1.924	-59.6063	1.00
1.974	-59.6096	0.99
2.024	-59.6110	0.97_4
2.034	-59.6111	0.97_2
2.044	-59.6111_6	0.97
2.054	-59.6111_8	0.96_9
2.064	-59.6111_6	0.96_8
2,074	-59.6111	0.96_7
2.124	-59.6104	0.96_3
E_1	-59.5764	
E_2	-59.5872	

TABLE 10

The calculated and observed spin density, in units of 10^{24} cm^{-3}, at various nuclei in the tetramer structures VIII, IX and X.

Structure	Nucleus	$R_{ns\ ns}$	ρ_{calc}	ρ_{total}	$\rho_{total}^{(obs)}$
VIII	H'	0.0572	0.130	0.668	0.169,[20]
	H	0.0163	0.037		0.140[55]
IX	H'	0.0459	0.105	0.816	
	H	0.0433	0.099		
X	N	0.0677	1.505	6.018	6.440 [15]
	H	0.0325	0.074	0.888	-0.072

TABLE 11

The calculated and observed ESR linewidths for the hydrated and ammoniated electrons for a range of correlation times.

Solvent	Structure	T(°K)	τ_c(psec)	δH_{calc}	δH_{obs}
H_2O	VIII	278	13.6	0.25	<0.5 [46]
D_2O	VIII	278	13.6	0.015	
H_2O	IX	278	13.6	0.28	
D_2O	IX	278	13.6	0.017	
NH_3	X	293	4.8	0.22	0.025 [37]
			0.96	0.045	
ND_3	X	293	4.8	0.15	
			0.96	0.031	
			5.76	0.18	
			1.15	0.037	

TABLE 12.

Some experimental and computed properties for the ammoniated and hydrated electrons.

	Ammonia (240°K)		Water (300°K)	
	Obs.	Calc.	Obs.	Calc.
E_{max} (eV)	0.80	0.72	1.72	2.08
$dE_{max}/dT \times 10^3$ eV/°K	-1.5±0.2	-2.0	-2.9	-4.0
Half-bandwidth (eV)	0.46	0.08	0.92	0.1
ESR linewidth (gauss)	0.025	0.045	0.5	0.25
ΔV ml/mole	84±15	81	1-6	30.19

References to Chapter 4.

1. J.L. Dye, Metal-Ammonia Solutions, Eds. J.J. Lagowski, M.J. Sienko, p.1, Butterworths, London (1970).
2. J. Kaplan and C. Kittel, J.Chem.Phys., 21, 1429 (1953).
3. A.H. Kahn and C. Kittel, Phys.Rev., 89, 315 (1953).
4. M. Natori and T. Watanabe, J.Phys.Soc.,(Japan), 21, 1573 (1966); M. Natori, J.Phys.Soc. (Japan), 24, 913 (1968), 27, 1309 (1969).
5. W.C. Gottschall and E.J. Hart, J.Phys.Chem., 71, 2102 (1967).
6. L. Raff and H.A. Pohl, Solvated Electron,Adv. Chem. Ser. 50 Ed. R.F. Gould, p.173 (1965).
7. M. Weissmann and N.V. Cohan, Chem.Phys.Lett., 7, 445 (1970).
8. D. Eisenberg and W. Kauzmann, The Structure and Properties of Water, p.115, Clarenden Press, Oxford (1968).
9. B.J. McAloon and B.C. Webster, Theor.Chim.Acta., 15, 385 (1969).
10. R.K. Quinn and J.J. Lagowski, J.Phys.Chem., 73, 2326 (1969).
11. Y.G. Gurikov, J.Struct.Chem., 9, 523 (1968).
12. R.F. Kruh and J.I. Petz, J.Chem.Phys., 41, 891 (1964).
13. G.V. Buxton, F.S. Dainton, T.E. Lantz and F.P. Sargent, Trans.Faraday Soc., 66, 2962 (1970).
14. I. Eisele, R. Lapple and L. Kevan, J.Amer.Chem.Soc., 91, 6504 (1969); I. Eisele and L. Kevan, J.Chem.Phys., 53, 1867 (1970).
15. R. Catterall, ref.1, p.105.
16. L. Kevan, Radiation Chemistry of Aqueous Systems, Ed. G. Stein, p.21, Wiley, London (1968).
17. I.A. Taub and K. Eiben, J.Chem.Phys., 49, 2499 (1968).
18. K. Kawabata, J.Chem.Phys., 55, 3672 (1971).
19. K. Eiben and D. Schulte-Frohlinde, Z.Phys.Chem., 45, 20 (1965).
20. P.N. Moorthy and J.J. Weiss, Phil.Mag., 10, 659 (1964); L. Kevan, J.Amer.Chem.Soc., 87, 1481 (1965); B.G. Ershov, O.Y. Grinberg and Y.S. Lebedev, J.Struct.Chem., 9, 603 (1968); C. Lifshitz and G. Stein, J.Chem.Phys., 42,3330 (1965).
21. B.D. Michael, E.J. Hart and K.H. Schmidt, J.Phys.Chem., 75, 2798 (1971).
22. S. La Placa and B. Post, Acta.Cryst., 13, 503 (1960).
23. G. Nilsson, J.Chem.Phys., 56, 3427 (1972).
24. M.G. Robinson, K.N. Jha and G.R. Freeman, J.Chem.Phys., 55, 4933 (1971); R.R. Hentz, Farhataziz and E.M. Hansen, J.Chem.Phys, 55, 4974 (1971).

25. U. Schindewolf, R. Vogelsgesang and K.W. Boddeker, Angew.Chem. Int.Ed. (English), 6, 1076 (1967);
U. Schindewolf, H. Kohrmann and G. Lang, Angew.Chem.Int.Ed. (English), 8 512 (1969).
26. J.P. Keene, Rad.Res., 22, 1 (1964);
E.J. Hart, Ann.Rev.Nucl.Sci., 15, 125 (1965).
27. D.A. Copeland, N.R. Kestner and J. Jortner, J.Chem.Phys., 53, 1189 (1970).
28. P.F. Rusch, W.H. Koehler and J.J. Lagowski, ref. 1, p. 41.
29. W.H. Hamill, J.Chem.Phys., 53, 473 (1970).
30. R.R. Hentz and D.W. Brazier, J.Chem.Phys., 54, 2777 (1971).
31. R. Catterall and N.F. Mott, Adv.Phys., 18, 665 (1970).
32. S. Arai and M.C. Sauer, J.Chem.Phys., 44, 2297 (1966).
33. J.L. Dye, M.G. DeBacker and L.M. Dorfman, J.Chem.Phys., 52, 6251 (1970).
34. B.J. Brown, N.T. Barker and D.F. Sangster, J.Phys.Chem., 75, 3639 (1971).
35. A. Ekstrom and J.E. Willard, J.Phys.Chem., 72, 4599 (1968).
36. D.E. O'Reilly, J.Chem.Phys., 41, 3736 (1964);
K. Fueki, J.Chem.Phys., 45, 183 (1966).
37. C.A. Hutchison and R.C. Pastor, J.Chem.Phys., 21, 1959 (1953).
38. K.D. Vos and J.L. Dye, J.Chem.Phys., 38, 2033 (1963).
39. H.M. McConnell and C.H. Holm, J.Chem.Phys., 26, 1517 (1957).
40. C.A. Hutchison and D.E. O'Reilly, J.Chem.Phys., 34, 1279 (1961);
D.E. O'Reilly, J.Chem.Phys., 35, 1856 (1961).
41. V.L. Pollak, J.Chem.Phys., 34, 864 (1961).
42. R.A. Newmark, J.C. Stevenson and J.S. Waugh, J.Chem.Phys., 46, 3514 (1967);
C. Lambert, ref. 1, p. 301.
43. M.F. Deigen and S.I. Pekar, Zh.Eksp.Teor.Fiz., 34, 684 (1958).
44. M.J. Blandamer, L. Shields and M.C.R. Symons, Nature, 60, 726 (1963), J.Chem.Soc., 4352 (1964);
L. Kevan, J.Amer.Chem.Soc., 87, 1481 (1965).
45. M.J. Blandamer, L. Shields and M.C.R. Symons, J.Chem.Soc., 1127 (1965).
46. E.C. Avery, L.R. Remko and B. Smaller, J.Chem.Phys., 49, 951 (1968).
47. A.F. Kip, C. Kittel, R.A. Levy and A.M. Portis, Phys.Rev., 91, 1066 (1953).

48. N. Bloembergen, E.M. Purcell and R.V. Pound, Phys.Rev., 73, 679 (1948).
49. R. Catterall, L.P. Stodulski and M.C.R. Symons, ref. 1, p. 151.
50. P. Debye, Polar Molecules, Chem. Catalog. Co., New York (1929).
51. R. Meakins, Trans. Faraday Soc., 54, 1160 (1958);
D.A. Pitt and C.P. Smyth, J.Phys.Chem., 63, 582 (1959);
R.D. Nelson and C.P. Smyth, J.Phys.Chem., 68, 2704 (1964).
52. N.E. Hill, Proc.Phys.Soc., B67, 149 (1954);
A. von Gierer and K. Wirtz, Z. Naturforsch, 8a, 532 (1953).
53. E.H. Grant, J.Chem.Phys., 26, 1575 (1957).
54. J.A. Pople, D.L. Beveridge and P.A. Dobosh, J.Amer.Chem.Soc., 90, 4201 (1968).
55. J.E. Bennett, B. Mile and A. Thomas, J.Chem.Soc., A, 1393 (1967).
56. R. Catterall, M.C.R. Symons and J.W. Tipping, ref. 1, p. 317.

CONCLUSION.

The current theories of the solvated electron in polar liquids have been reviewed and a fresh approach, based on the proposal of molecular models, introduced. Although more calculations on other species are required to ascertain the profitability of the molecular approach, the model calculations described are very encouraging.

Both the semicontinuum treatment and the molecular approach give estimates for the same property, and fail in the bandwidth calculations. The molecular models do reveal features which are not accomodated within the semicontinuum treatment. The latter approach relies on molecular reorientation and polarisation to provide a potential well within which the electron is trapped. The degree of reorganisation is not readily ascertained.

The molecular approach, on the other hand, is immediately suited to accomodate the singularities in the potential experienced by the electron as well as the effects of molecular orientation. If molecular rearrangement or the existance of some defect site in the liquid is important for stabilisation, a molecular model is most likely to reveal the outstanding features.

The dimer model calculations proved to be useful in this context. By consideration of the relaxation of the dimer structure some observed and new spectral phenomena are predicted. The INDO calculations also showed that, for the hydrated electron, the most favourable molecular geometry of a tetramer structure is not that expected from an electrostatic model. The match between the computed properties for the cluster model VIII, and the observed properties of the hydrated electron demonstrates that this structure certainly deserves further study.

Contrary to the semicontinuum and cavity models, in the prescence of the excess electron, no conventional cavity is formed. The molecular model VIII of the hydrated electron contracts when the electron is introduced. Dilation phenomena are suggested to be a manifestation of lattice expansion. The test of this hypothesis awaits the investigation of more extensive molecular models.

Although the calculated ESR linewidths are of the correct order of magnitude, the spin densities at protons are larger than the observed values in solid media. This property may perhaps be better evaluated using a more accurate technique than the INDO method.